

Frequentist Inference for Semi-mechanistic Epidemic Models with Interventions

Heejong Bong

Department of Statistics, University of Michigan, Ann Arbor, MI, USA.

E-mail: hbong@umich.edu

Valérie Ventura

Department of Statistics & Data Science and Delphi Research Group, Carnegie Mellon University, Pittsburgh, PA, USA.

E-mail: vventura@stat.cmu.edu

Larry Wasserman

Department of Statistics & Data Science, Machine Learning Department and Delphi Research Group, Carnegie Mellon University, Pittsburgh, PA, USA.

E-mail: larry@stat.cmu.edu

Summary. The effect of public health interventions on an epidemic are often estimated by adding the intervention to epidemic models. During the Covid-19 epidemic, numerous papers used such methods for making scenario predictions. The majority of these papers use Bayesian methods to estimate the parameters of the model. In this paper we show how to use frequentist methods for estimating these effects which avoids having to specify prior distributions. We also use model-free shrinkage methods to improve estimation when there are many different geographic regions. This allows us to borrow strength from different regions while still getting confidence intervals with correct coverage and without having to specify a hierarchical model. Throughout, we focus on a semi-mechanistic model which provides a simple, tractable alternative to compartmental methods.

1. Introduction

We consider the problem of estimating epidemic models that include public health interventions. We use the term “intervention” very broadly to refer to any variable whose effect on the epidemic is of interest such as: mask usage, changes in social mobility, lockdowns, vaccines, etc. We focus on the semi-mechanistic model from Bhatt et al. (2023) which we describe in Section 2. The model provides a simple, tractable alternative to compartmental models (such as the SIR model of Kermack et al., 1927) but, as shown in Bhatt et al. (2023), it still captures enough dynamics to provide accurate modeling of the epidemic process.

During the Covid-19 epidemic, numerous papers used similar models for making scenario predictions; see, for example, Perra (2021); Gunaratne et al. (2022); Lazebnik et al. (2022); Vytla et al. (2021); Baker et al. (2020). Virtually all of these papers use Bayesian methods to estimate the parameters of the model. Typically, the posterior is approximated by Monte Carlo methods. Bayesian methods provide a powerful approach for combining prior information with data. But these methods do have some drawbacks (Bong et al., 2023). First, one has to specify many priors and the inference can be sensitive to the choice of priors. Second, Bayesian inferences do not come with frequency guarantees: a 95 percent posterior interval does not contain the true parameter value 95 percent of the time. Frequentist methods require no priors and have proper frequency guarantees.

Our comparisons of frequentist and Bayesian methods in this paper is not meant as a criticism of the Bayesian approach — which can be a powerful way to incorporate prior information — but

rather to provide methods to perform frequentist inferences and highlight the differences in the two approaches when modeling epidemics.

In some cases, we have data from several different regions. The accuracy of the estimates can be improved by properly combining the information from the different regions. In the Bayesian framework, information is combined by positing a hierarchical model. This can introduce bias if this model is mis-specified. We show how information can be combined in a frequentist manner in a way that does not require specifying a hierarchical model.

Related Work. The literature on inference for epidemic models is huge and we cannot provide a complete review here. In addition to the references mentioned earlier we also point to Chatzilena et al. (2019); Fintzi et al. (2022); Li et al. (2021) as recent examples of some of the approaches. Again we emphasize that almost all work uses Bayesian inference in contrast to our approach. The work in Bhatt et al. (2023) is the closest to ours and is, in fact, the main inspiration for our work.

Paper Outline. In Section 2 we describe the model and in Section 3 we describe how to fit the model to data by maximum likelihood (ML). It is important to check the model fit so that we can trust inferences about model parameters and derived forecasts, which we address in Section 4. In Section 5 we develop inference for ML estimates and scenario predictions, which are robust to model mis-specifications. In Section 6 we show how to use shrinkage methods to improve estimation when there are several different geographic regions, without having to specify a hierarchical model. In Section 7 we apply our methods to simulated and observational data. We conclude in Section 8.

2. The Semi-mechanistic Model for Infections, Outcomes and Treatments

Let Y_1, Y_2, \dots, Y_T denote a scalar time series of observed outcomes (such as deaths) at a location and $I_{-\infty}, \dots, I_0, I_1, \dots, I_T$ denote the associated process of new infections where t typically indexes days or weeks; we start their indexing at $-\infty$ because Y_t depends on infections in the past. The I_t 's are typically latent (unobserved) because they are difficult to measure. We use overlines to denote histories, for example, $\bar{I}_t = (I_{-\infty}, \dots, I_t)$ and $\bar{Y}_t = (Y_1, \dots, Y_t)$.

We focus on the model from Bhatt et al. (2023) which is

$$\begin{aligned}\mathbb{E}[Y_t | \bar{I}_t, \bar{Y}_{t-1}] &= \alpha_t \sum_{s:s < t} I_s \pi_{t-s} \\ \mathbb{E}[I_t | \bar{I}_{t-1}, \bar{Y}_{t-1}] &= R_t \sum_{s:s < t} I_s g_{t-s}\end{aligned}\tag{1}$$

for $t > 0$, where $g_r \geq 0$, $\sum_{t=1}^{\infty} g_t = 1$, is the generating distribution that specifies the probabilities of the possible lags between an infection and a secondary infection, and the lag between infection and outcome has distribution $\pi_r \geq 0$, with $\sum_{t=1}^{\infty} \pi_t = 1$. The ascertainment rate α_t is the probability that an infection at t leads to an outcome and the reproduction number $R_t > 0$ is the mean number of infections generated in the future by an infection at t . The reproduction number is typically the parameter of main interest because it quantifies the progression of the epidemic. Finally, as is standard in time series analyses, the expectations are with respect to the conditional distributions of Y_t and I_t given the past. These distributions are often assumed to be Poisson or Negative Binomial (NB), the latter being more flexible and having the former as a limiting case.

This model, in its general form, where g and π are unknown, and α_t and R_t can vary with t , is not identified, as there are more parameters than data points. Hence there is no consistent estimator of the parameters. Typically, g and π are estimated separately, which we assume as well. Hence, we take them as fixed in the rest of the paper; they are plotted in Fig. 2. Similarly, α_t is also typically estimated from other data sources. Finally, to be able to estimate

the reproduction number R_t consistently, one needs to assume a model with a finite number of degrees of freedom, for example $R_t = \sum_{j=1}^k \gamma_j b_j(t)$ for basis functions b_1, \dots, b_k .

Now let $A_{-\infty}, \dots, A_0, A_1, \dots, A_T$ represent a scalar or vector time series of some interventions such as mobility, masks, vaccines, lockdowns etc. To model the effect of this intervention we will modify the model to include the A_t 's. (There are other ways to model the intervention such as marginal structural models; see Bonvini et al., 2022). We consider the model in Bhatt et al. (2023):

$$\mathbb{E}[I_t | \bar{I}_{t-1}, \bar{Y}_{t-1}, \bar{A}_t] = R(\bar{A}_t, \beta) \sum_{s:s < t} I_s g_{t-s}, \quad (2)$$

where $\bar{A}_t = (A_{-\infty}, \dots, A_t)$ and $R(\bar{A}_t, \beta)$ is some parametric model with the property that it does not depend on A when β (or some component of β) is 0. This model assumes that the reproduction number changes only through the interventions, which is reasonable if the period of study is short enough that conditions other than the interventions – e.g. the prevalence of population immunity, number of susceptibles, etc. – that can affect disease transmission remain unchanged. The parametrization used in Bhatt et al. (2023) is

$$R_t \equiv R(\bar{A}_t, \beta) = K \left(1 + e^{-(\beta_0 + \beta_1^\top A_t)} \right)^{-1}, \quad (3)$$

where $\beta = (\beta_0, \beta_1)$, K is the maximum possible transmission rate and A_t is a vector representing one or several interventions. That is, R_t/K is modelled as the logistic function of $(\beta_0 + \beta_1^\top A_t)$. Note that β_1 measures the change in the reproduction number R_t with respect to changes in A_t , but it is hard to interpret it more meaningfully because the logistic function is non-linear in A_t . We can, however, look at R_t itself, which is more interpretable. We discuss this point more in Section 7.2. (In the application of Section 7.2, $\beta_1^\top A_t$ is not sufficiently small to linearize the logistic function.) An alternative to the reproduction number in Eq. (3) would be to include the intervention in the sum, leading to the exponential model used in Bonvini et al. (2022)

$$\mathbb{E}[I_t | \bar{I}_{t-1}, \bar{Y}_{t-1}, \bar{A}_t] = \sum_{s:s < t} e^{\beta_0 + \beta_1^\top A_s} I_s g_{t-s}.$$

In either case, the assumption is that the intervention A affects the outcome Y by way of infections I , which is reasonable since Y , e.g. deaths or cases, cannot happen without infections. See Fig. 1. In the rest of the paper, we focus on the model in Eq. (3) so that our results can be compared to Bhatt et al. (2023).

Our two primary goals are to obtain point estimates and confidence intervals for β and R_t , so we can quantify the effects of interventions on the outcome, and use these estimates to produce scenario predictions.

Remark: *The parameter determines the local effect of A on R_t . But if we want the average treatment effect of the entire treatment vector a_1, \dots, a_T on the final value Y_T then one needs to use the g -formula Robins and Wasserman (1997); Bates et al. (2022).*

3. Estimation

Here we discuss maximum likelihood inference for the model parameters. We focus on one single observed time series but in Section 6 we consider shrinkage methods for dealing with time series at multiple locations. So far we have only specified the means of the infection and death processes in Eq. (1). To complete the model, we assume that the Y_t are either Gaussian or Negative Binomial (NB) distributed, but our methods can easily be extended to other distributions. Just as in Bhatt et al. (2023), we only model the distribution of the outcome and let the latent infection process be deterministic but unobserved, which implies that the Y_t are independent conditional on its past \bar{Y}_{t-1} . This is an unrealistic assumption – infections are random – but

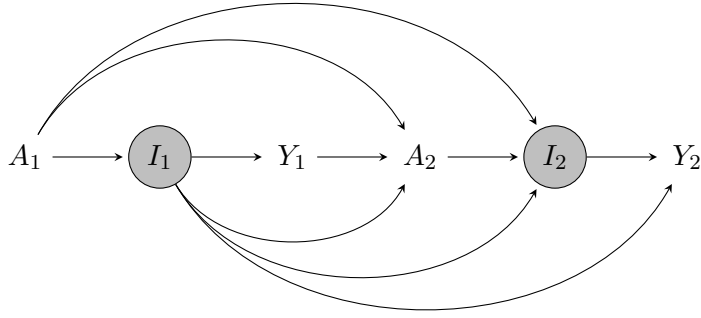


Fig. 1. DAG for the model. Note that A affects Y only through I .

because we observe only one repeat of the outcome process, we cannot identify the distributions of both I_t and Y_t . Therefore, instead of fitting Eq. (1), we fit

$$\begin{aligned} \mathbb{E}[Y_t | \bar{I}_t, \bar{Y}_{t-1}, \bar{A}_t] &= \mathbb{E}[Y_t | \bar{A}_t] = \alpha_t \sum_{s:s < t} I_s \pi_{t-s} \\ I_t &= R(\bar{A}_t, \beta) \sum_{s:s < t} I_s g_{t-s} \end{aligned} \quad (4)$$

where Y_t is either Gaussian or NB. Both distributions have an additional nuisance parameter ν_t , the standard deviation parameter for the Gaussian distribution and the inverse dispersion parameter for the NB distribution. We assume $\nu_t = \nu$ for all t . The parameter to be estimated is $\theta = (\beta, \nu, \mu)$, where β is the reproduction number parameter, ν is the nuisance parameter and μ is the seeding value, described below. We obtain the maximum likelihood estimator (MLE) of θ using the Block Coordinate Descent Algorithm described in Appendix A.

Infection process seeding The expectation of Y_t in Eq. (4) depends on all infections I_t prior to time t . Because Y_t is observed for $t \geq 1$, we cannot infer I_t prior to $t = 1$. Bhatt et al. (2023) thus assumed $I_t = 0$ for $t \leq -T_0$ and $I_t = e^\mu$ for $t = -T_0 + 1, \dots, 0$, where μ is a parameter to be estimated and $T_0 = 6$. We proceeded similarly but with $T_0 = 40$, because the infection-to-death distribution π in Fig. 2 has substantial mass on $\{1, \dots, 40\}$, and we obtained better fits than with $T_0 = 6$, especially for small t .

Note that the chosen “seeding” does not conform with the data or the model – infections cannot remain constant over time – which induces some bias. We initially tried seeding only one value at time $-T_0$, specifically $I_{-T_0} = e^\mu$, with μ and T_0 to be estimated, and $I_t = 0$ for $t \leq -T_0$. But because there is little information in the data about I_t for $t \leq 0$, this approach produced very large confidence intervals for the parameters, so we abandoned it. The optimal seeding strategy involves a bias-variance tradeoff and remains an open problem.

Parameter identifiability We deal with the nonidentifiability that arises from having too many parameters by imposing restrictions such as taking $\alpha_t = \alpha$ to be constant and assuming that R_t varies with t only through A_t . Both these assumptions are reasonable for the data analysis in Section 7.2 because the study period is short enough that α_t and R_t would not naturally vary on their own. Otherwise one could include a time varying intercept with a small number of parameters in the model for R_t , as in Bonvini et al. (2022). In the Bayesian framework, it is not uncommon to ignore the identifiability issues since, formally, the posterior can be computed even when there is nonidentifiability. But this is dangerous because then the posterior is driven by the

prior even with an infinite sample size. The effect of the nonidentifiability is then hidden from the user. However, there are methods to deal with identifiability issues in Bayesian inference; see Gustafson (2015); Giacomini and Kitagawa (2021).

PROPOSITION 3.1. *Assume that the data follow model (4) and that Y_t given $(\bar{I}_T, \bar{Y}_{t-1}, \bar{A}_t)$ is either Gaussian or Negative Binomial with dispersion parameter ν . Also assume that (a) if $\beta \neq 0$ then $P(\beta_0 + \beta_1^\top A_t = 0, \text{ for all } t = 1, \dots, T - T_0) = 0$ and (b) $\sum_{t=1}^{T_0} \pi_t > 0$ and $\sum_{t=1}^{T_0} g_t > 0$. Then $\theta = (\beta, \nu, \mu)$ is identified.*

The proof is in Appendix B. Condition (a) requires that $\beta_0 + \beta_1^\top A_t$ not always be 0, which is a very weak assumption. The generating and infection-to-death distributions g and π (Fig. 2) satisfy condition (b) for any small T_0 – in fact the sums are close to 1 for $T_0 = 40$.

4. Model Checking

It is important to check the adequacy of the regression mean so that we can trust inferences about model parameters, and while we could set confidence intervals for parameters based on the asymptotic normal distribution of ML estimates, checking the distribution of the data is also important because epidemiological models are often used to forecast the future time course of epidemics (see Section 5).

Regression methods provide a battery of diagnostics to assess model fit and identify outliers and influential observations. Because our model assumes that the latent infection process is deterministic, it implies that the observed deaths are independent conditional on the past. Hence our model fits within the regression framework, although we cannot write analytically the regression mean. We can nevertheless apply standard diagnostics.

Most diagnostics are based on residuals. For non-Gaussian data, deviance residuals are close to normally distributed, and therefore more appropriate for diagnostics, than raw residuals, although they are comparable when the outcome count data are large. For brevity and simplicity here, we therefore focus on raw residuals. They are defined as $e_t \equiv Y_t - \hat{Y}_t$, where $\hat{Y}_t = \mathbb{E}_{\hat{\theta}}[Y_t | \bar{A}_t]$.

Standardized residuals are given by $r_t = e_t / \sqrt{(1 - h_t) \widehat{\text{Var}}(Y_t)}$, where $\widehat{\text{Var}}(Y_t) = \hat{\nu}^2 = n^{-1} \sum (Y_t - \hat{Y}_t)^2$ for Gaussian data, $\widehat{\text{Var}}(Y_t) = \hat{Y}_t (\hat{Y}_t^2 / \nu)$ for NB data, and h_t is the leverage of observation t , obtained from the diagonal of the hat matrix, that is, the projection matrix corresponding to the linearization at the MLE. We have no explicit hat matrix here, but because the covariates, time and intervention(s), are equally spaced for the former and designed or taking values in a range for the later, all observations should have similar, and thus very small, leverage, so that $(1 - h_t) \approx 1$ for all t . Studentized residuals are defined like standardized residuals, except that to obtain the residual for Y_t , all parameters are estimated without Y_t .

Model diagnostics aim to assess the adequacy of the regression mean function and the assumed distribution of the data. For the former we plot the standardized residuals versus all covariates and fitted values – they should look random and homoskedastic – and for the later, we produce a Q-Q plot of the standardized residuals versus the standard normal quantiles.

Case diagnostics aim to identify influential points, that is, points that have large influence on parameter estimates, measured by Cook’s distance:

$$D_t = \sum_{t=1}^T (\hat{Y}_t - \hat{Y}_{(-t)})^2 / (ps^2),$$

where $s^2 = \sum (Y_t - \hat{Y}_t)^2 / (n - p)$, p is the number of parameters, and the subscript $(-t)$ indicates that estimates were obtained without Y_t . A value of D_t larger than one usually signals influence.

Large values of $C_t = (\hat{\beta}_1 - \hat{\beta}_{1,(-t)}) / \sqrt{\text{Var}(\hat{\beta}_1)}$ more specifically detect points that influence $\hat{\beta}_1$, and similarly for other β_j ’s if there are several interventions. Influential points are either high

leverage points – but there shouldn't be any since $h_t \approx 0$ for all t – or outliers, so it is also useful to identify outliers using standardized residuals.

5. Model Free Standard Errors, CLT and Confidence Set

We now turn to the issue of obtaining standard errors and confidence sets for parameter $\theta = (\beta, \nu, \mu)$ defined in Section 3. Note that under model misspecification, the stochastic process \bar{Y}_T may exhibit temporal dependence conditional on \bar{I}_T . We want an estimate of the standard error that is robust to extra dependence of this sort. In order to establish consistency and asymptotic normality of the MLE under this setting, we require that the process has a sufficiently fading memory as discussed by Pötscher and Prucha (1997). As an illustration, we will assume that \bar{Y}_T is well-approximated by an α -mixing process, which is a class of random processes that have the suitable “fading memory” property; see Chapter 6 in Pötscher and Prucha (1997), and below for the definitions of (a) α -mixing processes and (b) the concept of approximation.

DEFINITION 5.1. Let \bar{Y}_T be a stochastic process on a probability space $(\mathbb{R}, \mathfrak{F}, \mathbb{P})$.

(a) Define

$$\alpha(j) = \sup_{k \in \mathbb{N}} \sup \{ |\mathbb{P}[F \cap G] - \mathbb{P}[F]\mathbb{P}[G]| : F \in \mathfrak{F}_{[1,k]}, G \in \mathfrak{F}_{[k+j,T]} \},$$

where $\mathfrak{F}_{[t,s]}$ is the σ -field generated by Y_t, \dots, Y_s for $1 \leq t < s \leq T$. If $\lim_{j \rightarrow \infty} \alpha(j) = 0$, we say that the process (Y_t) is α -mixing.

(b) Let $(Y_t^o \in \mathbb{R}^p : t = -\infty, \dots, \infty)$ be a random process we take as a baseline. We say \bar{Y}_T is near epoch dependent of size $-q$ on the baseline process Y_t^o if

$$\sup_t \mathbb{E}[|Y_t - \mathbb{E}[Y_t | Y_{t-m}^o, \dots, Y_{t+m}^o]|^2] = O(m^{-2q}).$$

The rest of this section relies heavily on Pötscher and Prucha (1997) Theorems 7.1 and 11.2, and associated assumptions. The theorems entail consistency and asymptotic normality of our estimator conditional on \bar{A}_T , so our assumptions below are presented under the σ -algebra $\mathfrak{F}(\bar{Y}_T)$ generated by \bar{A}_T . First, we make the following two assumptions on \bar{Y}_T .

ASSUMPTION 5.2. Conditional on \bar{A}_T , \bar{Y}_T is near epoch dependent of size $-2(\gamma - 1)/(\gamma - 2)$ on an α -mixing baseline process with mixing coefficients $\alpha(j) = O(j^{-2\gamma/(\gamma-2)})$ for some $\gamma > 2$, almost surely.

ASSUMPTION 5.3. For $\gamma > 2$ in Assumption 5.2, there exists $\mathfrak{F}(\bar{A}_T)$ -measurable random variable $Y_{4\gamma, \max} \in (0, \infty)$ such that

$$\sup_t \mathbb{E}[Y_t^{4\gamma} | \bar{A}_t] \leq Y_{4\gamma, \max}, \text{ a.s.}$$

and the conditional distributions of Y_t on \bar{A}_t satisfy tightness property, i.e.,

$$\lim_{m \rightarrow \infty} \sup_T T^{-1} \sum_{t=1}^T \mathbb{P}[Y_t \notin K_m | \bar{A}_t] = 0, \text{ a.s.},$$

for some sequence of $\mathfrak{F}(\bar{A}_T)$ -measurable random compact sets $K_m \subset \mathbb{R}$.

Assumption 5.2 requires that the correlations between the residuals die off at a polynomial rate as the observations get further apart in time. Some assumption of this form is used in most time series analysis. This assumption appears to be met in the data analysis in Section 7.2; see

Appendix Fig. 19. Assumption 5.3 further requires that certain moments are bounded, which is automatically satisfied if the random variables are bounded, which they are in Section 7.2.

Next, we need an identifiability assumption. In Theorem 3.1, we made a weak one in assumption (a), but we need a stronger one for the consistency and asymptotic normality of the MLE.

ASSUMPTION 5.4. There exists $t \in \{1, \dots, T_0\}$ such that $\pi_t > 0$, and $\pi_t = g_t = 0$ for any $t \geq \tau$ for some $\tau < T$. Furthermore, there exists $\mathfrak{F}(\bar{A}_T)$ -measurable random variables $\lambda_{\min, A}$ and A_{\max} such that $0 < \lambda_{\min, A} \cdot \|\beta\|_2^2 \leq \frac{1}{T-t} \|\beta^\top (A_{t+1}, \dots, A_T)\|_2^2$ and $\|A_t\|_2 \leq A_{\max}$ for any $0 < t < T$ and β , almost surely.

This assumption holds with probability one if A has a continuous distribution. This is like the usual assumption that the design matrix in regression is non-singular.

Next, we define a parameter space Θ as follows.

DEFINITION 5.5. For given constants $I_{\min}, I_{\max}, D_{\max}^{(1)}, D_{\max}^{(2)} > 0, r_{\min}$ and r_{\max} , let Θ be a $\mathfrak{F}(A)$ -measurable random set of $\theta \equiv (\beta, \mu, \nu)$ such that

- (a) $0 < I_{\min} \leq \mathbb{E}_\theta [I_t | \bar{A}_t] \leq I_{\max} < \infty$ for all $t \geq 1$,
- (b) $\|\nabla_{(\beta, \mu)} \mathbb{E}_\theta [I_t | \bar{A}_t]\|_\infty \leq D_{\max}^{(1)}, \|\nabla_{(\beta, \mu)}^2 \mathbb{E}_\theta [I_t | \bar{A}_t]\|_\infty \leq D_{\max}^{(2)}$ for any $t \geq 1$, and
- (c) $0 < r_{\min} \leq \frac{\sum_{t=1}^T \text{Var}_\theta [Y_t | \bar{A}_t]}{\sum_{t=1}^T \mathbb{E}_\theta [Y_t | \bar{A}_t]} \leq r_{\max}$ for all $T \geq 1$,

almost surely.

Parameters in Θ satisfy that I_t and its derivatives have bounded moments given \bar{A}_t . It automatically holds if I_t is bounded, which is the case in the data analysis in Section 7.2.

Let $\ell(\theta) \equiv \sum_{t=1}^T \ell_t(\theta)$ denotes the log-likelihood function, where $\ell_t(\theta) \equiv \log p_{Y_t}(Y_t | \bar{I}_t, \bar{Y}_{t-1}, \bar{A}_t, \theta)$ ($= \log p_{Y_t}(Y_t | \bar{A}_t, \theta)$ since the I_t are assumed to be deterministic). Let $\hat{\theta} \equiv \arg \max_{\theta \in \Theta} \ell(\theta)$. Also define $\ell^*(\theta) \equiv \mathbb{E}[\ell(\theta) | \bar{A}_T]$. Because our model in Eq. (4) is nonlinear, the convexity of $\ell^*(\theta)$ and hence the uniqueness of the global maximum are not guaranteed. We assume that the global maximum is identifiably unique. The assumption is common in the consistency proof of MLEs (Pötscher and Prucha, 1997; van der Vaart, 2000).

ASSUMPTION 5.6. ℓ^* has an identifiably unique maximizer θ^* in Θ , almost surely. That is, θ^* is in the interior of Θ , and for every $\epsilon > 0$,

$$\liminf_{n \rightarrow \infty} \left[\inf_{\theta \in \Theta: \|\theta - \theta^*\|_2 \geq \epsilon} \ell^*(\theta) - \ell^*(\theta^*) \right] > 0.$$

We further assume that

$$\begin{aligned} \liminf_{T \rightarrow \infty} \lambda_{\min} \left(-\frac{1}{T} \nabla_{\theta}^2 \ell^*(\theta^*) \right) &> 0, \\ \liminf_{T \rightarrow \infty} \lambda_{\min} \left(\frac{1}{T} \cdot \text{Var} [\nabla_{\theta} \ell(\theta^*) | \bar{A}_T] \right) &> 0, \end{aligned}$$

almost surely.

Note that θ^* is defined conditional on \bar{A}_T , so θ^* is a $\mathfrak{F}(\bar{A}_T)$ -measurable random variable. If model correctly specifies the data generation, θ^* is essentially constant at the *true* value.

We now have all the elements to proceed with the normality and consistency of the MLE of $\theta = (\beta, \mu, \nu)$.

THEOREM 5.7. *Under Assumptions 5.2, 5.3, 5.4 and 5.6,*

$$T^{1/2}\Upsilon^{-1/2}(\hat{\theta} - \theta^*) \xrightarrow{d} \mathbf{N}(0, id),$$

where $\Upsilon \equiv (\mathbb{E}[H(\theta^*)|\bar{Y}_T])^{-1}\mathbb{E}[s(\theta^*)s(\theta^*)^\top|\bar{Y}_T](\mathbb{E}[H(\theta^*)|\bar{Y}_T])^{-1}$, $s(\theta) \equiv \nabla_\theta \ell(\theta)$ is the score function and $H(\theta)$ is the Hessian matrix of $\ell(\theta)$.

The proof of Theorem 5.7 is in Appendix B.1. To construct confidence intervals, we need to estimate the variance matrix Υ . A plug-in estimator is

$$\hat{\Upsilon} = [H(\hat{\theta})]^{-1}s(\hat{\theta})s(\hat{\theta})^\top[H(\hat{\theta})]^{-1}.$$

However, this estimator does not have full rank. If $\nabla_\theta \ell_t(\hat{\theta})$ for $t = 1, \dots, T$ are mutually independent, then $\sum_{t=1}^T \nabla_\theta \ell_t(\hat{\theta})\nabla_\theta \ell_t(\hat{\theta})^\top$ is a consistent estimator of $\mathbb{E}[s(\theta^*)s(\theta^*)^\top|\bar{Y}_T]$. But because there may be dependence due to model mis-specification, we instead use the heteroskedasticity and autocorrelation consistent (HAC) estimator (Newey et al., 1987):

$$\hat{S} \equiv \sum_{t,s \in (0,T]} w(|t-s|, T) \cdot \nabla_\theta \ell_t(\hat{\theta})\nabla_\theta \ell_s(\hat{\theta})^\top,$$

where w is a weight function satisfying $\lim_{T \rightarrow \infty} w(t, T) = 1$ for any fixed t . In particular, we set $w(t, T) = \max\{1 - |t|/\tau, 0\}$ where $\tau = \lfloor 4(T/100)^{2/9} \rfloor$. (This is a commonly used default value.) The resulting estimator,

$$\hat{\Upsilon} \equiv [H(\hat{\theta})]^{-1}\hat{S}[H(\hat{\theta})]^{-1},$$

is usually referred to as a *sandwich estimator*.

PROPOSITION 5.8. *Suppose that $\mathbb{E}[\nabla_\theta \ell_t(\theta^*)|\bar{A}_t] = 0$ at each t with probability 1. Under Assumptions 5.2, 5.3, 5.4 and 5.6, $\hat{\Upsilon}$ is a consistent estimate of Υ .*

The proof of Proposition 5.8 is in Appendix B.1. For Normal and NB models, the additional assumption stated in Theorem 5.8 implies that $\mathbb{E}[Y_t|\bar{A}_t] = \mathbb{E}_{\theta^*}[Y_t|\bar{A}_t]$. That is, for our inference based on the HAC variance estimate to work, the mean of Y_t must be correctly specified for each t ; distributional misspecifications do not affect the validity of the inference. This assumption is dubious in the data analysis of Section 7.2 because the residual diagnostics in Fig. 9 show some lack of fit at the start and end of the epidemic.

It follows that an asymptotic joint $1 - \alpha$ confidence interval for θ is

$$\begin{aligned} \mathcal{C} &= \hat{\theta} + \chi_{d,\alpha} \cdot T^{-1/2}\hat{\Upsilon}^{1/2}\mathcal{B}_d \equiv \{\hat{\theta} + \chi_{d,\alpha} \cdot T^{-1/2}\hat{\Upsilon}^{1/2}x : x \in \mathcal{B}_d\} \\ &= \{\theta : (\theta - \hat{\theta})^T \hat{\Upsilon}^{-1}(\theta - \hat{\theta}) \leq T^{-1}\chi_{d,\alpha}^2\}, \end{aligned}$$

where $\chi_{d,\alpha}$ is the α -quantile of the chi-square distribution with degree of freedom d , $\hat{\Upsilon}^{1/2}$ is the matrix square-root of $\hat{\Upsilon}$, and $\mathcal{B}_d \equiv \{x \in \mathbb{R}^d : \|x\|_2 \leq 1\}$ is the d -dimensional unit ball. Under model misspecification, the MLE is a consistent estimate of the distribution closest to the true distribution in Kullback-Leibler distance. The sandwich estimator is still valid in this case.

Global Confidence Bands for Scenario Predictions Having obtained a $(1 - \alpha)$ joint confidence set \mathcal{C} for θ , we can make scenario forecasts as follows. We fix A_1, \dots, A_T . Define

$$l_t = \min_{\theta \in \mathcal{C}} \mathbb{E}_\theta[Y_t|\bar{A}_t]$$

and

$$u_t = \max_{\theta \in \mathcal{C}} \mathbb{E}_\theta[Y_t|\bar{A}_t].$$

It follows that, under the scenario (A_1, \dots, A_T) ,

$$P(l_t \leq \mathbb{E}[Y_t] \leq u_t \text{ for all } t) \geq 1 - \alpha.$$

Remark. We can also construct prediction bands for Y_t rather than for the mean. We find that these tend to be very large. If one uses Bayesian prediction bands with strong priors, it is possible to obtain narrow prediction bands but these are very dependent on the prior and the distributional assumptions on Y_t .

6. Shrinkage: Borrowing strength across locations

Suppose now that we have data from N different geographic regions with corresponding parameters $\theta_{[1]}, \dots, \theta_{[N]}$. We would like to estimate each $\theta_{[j]}$ while taking advantage of any similarity between the parameters. This is usually done by shrinking the individual estimates towards each other which reduces the mean squared error of the estimators (James and Stein, 1960). One approach to shrinkage is to use a hierarchical model where we treat the $\theta_{[j]}$'s as draws from a distribution $g(\theta; \xi)$ depending on hyper-parameters ξ . For example, the R package `epidemia` (Scott et al., 2021) uses a Normal $(0, \Sigma)$ distribution. However, this requires specifying $g(\theta; \xi)$, which is difficult because the $\theta_{[j]}$'s are not observed. Instead, we use the approach from Armstrong et al. (2022) which provides a shrinkage method that does not require specifying this distribution. The method provides model-free confidence intervals for univariate parameters. In particular, this method corrects for the bias that is induced by shrinkage, which is important for getting correct frequentist coverage. Because our parameters $\theta_{[1]}, \dots, \theta_{[N]}$ are multivariate, we extend this method to the multivariate case.

Suppose that $\theta_{[1]}, \dots, \theta_{[N]} \in \mathbb{R}^d$ are drawn from some unknown distribution with mean θ_o and variance-covariance matrix $\Phi^{(2)}$ and that, conditional on $\theta_{[j]}$,

$$\widehat{\theta}_{[j]} | \theta_{[j]} \sim N(\theta_{[j]}, T_{[j]}^{-1} \Upsilon_{[j]}), \quad (5)$$

where $T_{[j]} = T_{[j]}(N)$ is the number of observed time points at region j , and $\Upsilon_{[j]} \in \mathbb{R}^{d \times d}$ is the $T_{[j]}$ -normalized variance matrix of the estimation error at region $j = 1, \dots, N$. This Normality assumption holds, at least approximately, due to the asymptotic Normality of the MLE. Define the shrinkage estimator

$$\widetilde{\theta}_{[j]} \equiv \theta_o + W_{[j]}(\widehat{\theta}_{[j]} - \theta_o), \quad (6)$$

where

$$W_{[j]} \equiv T_{[j]}(T_{[j]} \Upsilon_{[j]}^{-1} + \Phi^{(2)-1})^{-1} \Upsilon_{[j]}^{-1} = \Phi^{(2)}(\Phi^{(2)} + T_{[j]}^{-1} \Upsilon_{[j]})^{-1}.$$

For now, assume that θ_o and $\Phi^{(2)}$ are specified. Later, θ_o and $\Phi^{(2)}$ will be replaced by empirical estimates. (The estimator in Eq. (6) can be motivated by noting that it is the posterior mean of $\theta_{[j]}$ if $\theta_{[j]} \sim N(\theta_o, \Phi^{(2)})$. However, this distributional assumption is not used in what follows.)

While shrinkage has the effect of reducing the variance of the estimator to $T_{[j]}^{-1} \widetilde{\Upsilon}_{[j]}$ where $\widetilde{\Upsilon}_{[j]} \equiv W_{[j]} \Upsilon_{[j]} W_{[j]}$ (note that $W_{[j]} \preceq id$), it adds bias, and as a result, standard confidence intervals will not have correct coverage. Instead, consider a confidence region for $\theta_{[j]}$ of the form

$$\begin{aligned} \mathcal{C}_{[j]} &= \widetilde{\theta}_{[j]} + \chi \cdot T_{[j]}^{-1/2} \widetilde{\Upsilon}_{[j]}^{1/2} \mathcal{B}_d \equiv \{\widetilde{\theta}_{[j]} + \chi \cdot T_{[j]}^{-1/2} \widetilde{\Upsilon}_{[j]}^{1/2} x : x \in \mathcal{B}_d\} \\ &= \{\theta_{[j]} : (\theta_{[j]} - \widetilde{\theta}_{[j]})^T \widetilde{\Upsilon}_{[j]}^{-1} (\theta_{[j]} - \widetilde{\theta}_{[j]}) \leq T_{[j]}^{-1} \chi^2\} \end{aligned}$$

where $\chi > 0$, $\widetilde{\Upsilon}_{[j]}^{1/2}$ is the matrix square-root of $\widetilde{\Upsilon}_{[j]}$, $\mathcal{B}_d \equiv \{x \in \mathbb{R}^d : \|x\|_2 \leq 1\}$ is the d -dimensional unit ball.

If the model $\theta_{[j]} \sim N(\theta_o, \Phi^{(2)})$ were correct, we could use $\chi = \chi_{1-\alpha}$ where $\chi_{1-\alpha}^2$ is the $1 - \alpha$ quantile of χ^2 distribution with degree of freedom d . However, the resulting confidence set does

not have $1 - \alpha$ coverage in general. See Armstrong et al. (2022) for a detailed discussion in univariate cases. We instead use the approach by Armstrong et al. (2022). Conditional on $\theta_{[j]}$, the estimator $\tilde{\theta}_{[j]}$ has bias $\theta_o + W_{[j]}(\theta_{[j]} - \theta_o) - \theta_{[j]}$ and variance $T_{[j]}^{-1}W_{[j]}\Upsilon_{[j]}W_{[j]}^\top$. We define the normalized bias $b_{[j]}$ by

$$\begin{aligned} b_{[j]} &\equiv T_{[j]}^{1/2}(W_{[j]}\Upsilon_{[j]}^{1/2})^{-1}(\theta_o + W_{[j]}(\theta_{[j]} - \theta_o) - \theta_{[j]}) \\ &= T_{[j]}^{1/2}\Upsilon_{[j]}^{-1/2}(id - W_{[j]}^{-1})\epsilon_{[j]} = -T_{[j]}^{-1/2}\Upsilon_{[j]}^{1/2}\Phi^{(2)-1}\epsilon_{[j]}, \end{aligned}$$

where $\epsilon_{[j]} = \theta_{[j]} - \theta_o$. The non-coverage r_{d-1} of $\mathcal{C}_{[j]}$ depends only on the distribution of $\|b_{[j]}\|_2$:

$$r_{d-1}(\|b_{[j]}\|_2^2, \chi) \equiv \mathbb{P}[\|Z_d - b_{[j]}\|_2 \geq \chi|\theta_{[j]}] = \mathbb{P}[\chi_{d-1}^2 + (Z - \|b_{[j]}\|_2)^2 \geq \chi^2], \quad (7)$$

due to the symmetry of Z_d , where Z_d , χ_{d-1}^2 and Z are a d -dimensional standard Gaussian random vector, a Chi-squared random variable with degree of freedom $d - 1$ and a univariate standard Gaussian random variable. Now let

$$\rho_{m_{[j]}^{(2)}, m_{[j]}^{(4)}}(\chi) \equiv \sup_{F \in \mathcal{F}} \mathbb{E}_F[r_{d-1}(u, \chi)] \text{ such that } \mathbb{E}_F[u] = m_{[j]}^{(2)} \text{ and } \mathbb{E}_F[u^2] = m_{[j]}^{(4)}, \quad (8)$$

where $m_{[j]}^{(2)} = \mathbb{E}[\|b_{[j]}\|_2^2]$, $m_{[j]}^{(4)} = \mathbb{E}[\|b_{[j]}\|_2^4]$ and \mathcal{F} is the collection of all such probability distribution on $[0, \infty)$. That is, $\rho_{m_{[j]}^{(2)}, m_{[j]}^{(4)}}(\chi)$ is the maximum non-coverage of \mathcal{C}_j at each χ , subject to moment constraints. The moments of $\|b_{[j]}\|_2$ are calculated from the moments of $\theta_{[j]}$: if

$$\mathbb{E}[(\theta_{[j]} - \theta_o)(\theta_{[j]} - \theta_o)^\top] = \Phi^{(2)} \text{ and } \mathbb{E}[(\theta_{[j]} - \theta_o)^{\otimes 4}] = \Phi^{(4)},$$

where \otimes is the tensor product, the moments of $\|b_{[j]}\|_2$ are

$$\begin{aligned} m_{[j]}^{(2)} &= T_{[j]}^{-1} \text{tr} \left(\Upsilon_{[j]}^{1/2} \Phi^{(2)-1} \Upsilon_{[j]}^{1/2} \right) \\ m_{[j]}^{(4)} &= T_{[j]}^{-2} \sum_{i_1=1}^d \sum_{i_2=1}^d \Psi_{i_1, i_2}, \end{aligned} \quad (9)$$

where $\Psi_{i_1, i_2} \equiv \left\langle \Phi^{(4)}, (\Upsilon_{[j]}^{1/2} \Phi^{(2)-1})_{i_1}^{\otimes 2} \otimes (\Upsilon_{[j]}^{1/2} \Phi^{(2)-1})_{i_2}^{\otimes 2} \right\rangle$. As in univariate cases, $\rho_{m_{[j]}^{(2)}, m_{[j]}^{(4)}}$ can be estimated by numerically solving Eq. (8) with discretized support of $\|b_{[j]}\|_2$; see Appendix B of Armstrong et al. (2022). Finally, we define the critical value

$$\tilde{\chi}_{[j], 1-\alpha} \equiv \inf\{\chi : \rho_{m_{[j]}^{(2)}, m_{[j]}^{(4)}}(\chi) \leq \alpha\},$$

and define the confidence set

$$\tilde{\mathcal{C}}_{[j]} \equiv \tilde{\theta}_{[j]} + \tilde{\chi}_{[j], 1-\alpha} T_{[j]}^{-1/2} \tilde{\Upsilon}_{[j]}^{1/2} \mathcal{B}_d. \quad (10)$$

Since θ_o , $\Phi^{(2)}$ and $\Phi^{(4)}$ are unknown, we estimate them from $\hat{\theta}_{[1]} \dots \hat{\theta}_{[N]}$, and let $\hat{\theta}_o$, $\hat{\Phi}^{(2)}$ and $\hat{\Phi}^{(4)}$ be the estimates. Plugging the estimates in Eq. (10), we obtain the proposed empirical Bayesian confidence set.

The form of the shrinkage estimator was motivated by assuming that $\theta_{[j]} \sim N(\theta_o, \Phi^{(2)})$ but we show that $\tilde{\mathcal{C}}_{[j]}$ has the correct coverage without that assumption. Indeed, we do not even need to assume that $\theta_{[1, \dots, N]}$ are random. We instead formulate the coverage conditional on $\theta_{[1, \dots, N]}$ (and $\Upsilon_{[1, \dots, N]}$) which implies robustness of the coverage against prior misspecification.

As in Morris (1983), we say the confidence regions $\mathcal{C}_{[j]}$ has asymptotically $1 - \alpha$ average coverage intervals (ACIs) if

$$\liminf_{N \rightarrow \infty} \frac{1}{N} \sum_{j=1}^N \mathbb{P}[\theta_{[j]} \in \mathcal{C}_{[j]} | \theta_{[1, \dots, N]}, \Upsilon_{[1, \dots, N]}] \geq 1 - \alpha.$$

The asymptotic coverage relies on the conditional normality (Eq. (5)) of $\hat{\theta}_{[j]}$. Instead, we will only assume that $\hat{\theta}_{[j]}$ is asymptotically Normal with an estimated covariance matrix $\hat{\Upsilon}_{[j]}$ (in our case, $\hat{\Upsilon}_{[j]}$ in Theorem 5.8).

ASSUMPTION 6.1. $T_{[j]}(N) \rightarrow \infty$ as $N \rightarrow \infty$ so that the estimators are uniformly asymptotically Normal: given \mathcal{U} be the collection of balls in \mathbb{R}^d , suppose that

$$\lim_{N \rightarrow \infty} \max_{1 \leq j \leq N} \sup_{U \in \mathcal{U}} \left| \mathbb{P}[T_{[j]}^{1/2} \hat{\Upsilon}_{[j]}^{-1/2} (\hat{\theta}_{[j]} - \theta_{[j]}) \in U | \theta_{[1, \dots, N]}, \Upsilon_{[1, \dots, N]}] - \mathbb{P}[Z_d \in U] \right| = 0,$$

where Z_d is the d -dimensional standard Normal random variable.

ASSUMPTION 6.2. $\hat{\Upsilon}_{[j]}$ is consistent. That is, for every $\epsilon > 0$,

$$\lim_{N \rightarrow \infty} \max_{1 \leq j \leq N} \mathbb{P} \left[\|\hat{\Upsilon}_{[j]} - \Upsilon_{[j]}\|_2 \geq \epsilon \mid \theta_{[1, \dots, N]}, \Upsilon_{[1, \dots, N]} \right] = 0.$$

Another essential ingredient of the asymptotic coverage is the homoskedasticity of $\theta_{[j]}$ in the second and fourth moments. Because the theoretical argument is given conditional on $\theta_{[1, \dots, N]}$, we formulate and assume the homoskedasticity as follows.

ASSUMPTION 6.3. Suppose that $\sup_{[j]} \lambda_{\max}(\Upsilon_{[j]}) \leq \lambda_{\max, \Upsilon}$ for some $\lambda_{\max, \Upsilon} \in (0, \infty)$ and that \mathcal{U} is the collection of $d \times d$ positive semidefinite matrices Υ satisfying $\lambda_{\max}(\Upsilon) \leq \lambda_{\max, \Upsilon}$. We assume there exists θ_o such that $\hat{\theta}_o \rightarrow \theta_o$ in probability and $(\Phi^{(2)}, \Phi^{(4)})$ such that

$$\frac{1}{N_{\mathcal{X}}} \sum_{j: j \in \mathcal{I}_{\mathcal{X}}} (\theta_{[j]} - \theta_o)^{\otimes 2} \rightarrow \Phi^{(2)} \quad \text{and} \quad \frac{1}{N_{\mathcal{X}}} \sum_{j: j \in \mathcal{I}_{\mathcal{X}}} (\theta_{[j]} - \theta_o)^{\otimes 4} \rightarrow \Phi^{(4)}$$

as $N_{\mathcal{X}} \rightarrow \infty$ for any Borel set $\mathcal{X} \subseteq \mathcal{U}$, where $\mathcal{I}_{\mathcal{X}} \equiv \{j : \Upsilon_{[j]} \in \mathcal{X}\}$, $N_{\mathcal{X}} \equiv |\mathcal{I}_{\mathcal{X}}|$. In addition, we assume there exists $\lambda_{\min, \Phi}, \lambda_{\max, \Phi} \in (0, \infty)$ such that

$$\begin{aligned} \lambda_{\min, \Phi} &\leq \lambda_{\min}(\Phi^{(2)}) \leq \lambda_{\max}(\Phi^{(2)}) \leq \lambda_{\max, \Phi}, \\ \lambda_{\min, \Phi} &\leq \lambda_{\min}(\Phi^{(4)}) \leq \lambda_{\max}(\Phi^{(4)}) \leq \lambda_{\max, \Phi}. \end{aligned}$$

For brevity, let $\lambda_{\max, *} \equiv \max\{\lambda_{\max, \Upsilon}, \lambda_{\max, \Phi}, \lambda_{\min, \Phi}^{-1}\}$.

ASSUMPTION 6.4. Finally, we assume the estimates $\hat{\Phi}^{(2)}$ and $\hat{\Phi}^{(4)}$ are consistent.

$$\hat{\Phi}^{(2)} \xrightarrow{P} \Phi^{(2)} \quad \text{and} \quad \hat{\Phi}^{(4)} \xrightarrow{P} \Phi^{(4)} \quad \text{as } N \rightarrow \infty.$$

Theorem 6.5 shows that the average miscoverage of the confidence sets is α , asymptotically. The proof is in Appendix B.2.

THEOREM 6.5. *Under assumptions 6.1, 6.2, 6.3 and 6.4, for any Borel set $\mathcal{X} \subseteq \mathcal{U}$,*

$$\mathbb{E} \left[\frac{1}{N_{\mathcal{X}}} \sum_{j \in \mathcal{I}_{\mathcal{X}}} \mathbb{I}\{\theta_{[j]} \notin \tilde{\mathcal{C}}_{[j]}\} \mid \theta_{[1, \dots, N]}, \Upsilon_{[1, \dots, N]} \right] \leq \alpha + o(1),$$

where $\mathcal{I}_{\mathcal{X}} \equiv \{j : \Upsilon_{[j]} \in \mathcal{X}\}$, and $N_{\mathcal{X}} \equiv |\mathcal{I}_{\mathcal{X}}|$.

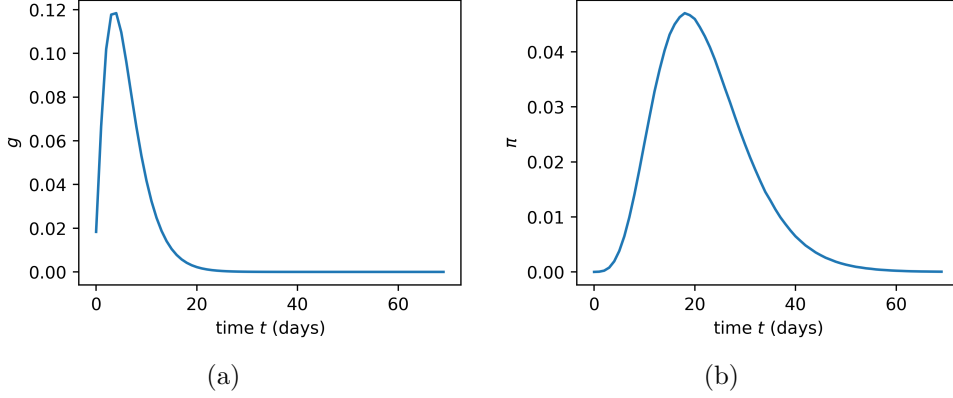


Fig. 2. Generating and infection-to-death distributions g and π from Bhatt et al. (2023).

We note that the average coverage result in Theorem 6.5 remains valid no matter the particular choice of $\hat{\theta}_o$, $\hat{\Phi}^{(2)}$ and $\hat{\Phi}^{(4)}$ provided that Assumption 6.4 holds. For the subsequent simulation study and data analysis, we use the *unconstrained* estimating scheme of Armstrong et al. (2022) (see Appendix A.1 therein); namely, we take

$$\hat{\theta}_o = \frac{\sum_j \xi_{[j]} \hat{\theta}_{[j]}}{\sum_j \xi_{[j]}}, \quad \hat{\Phi}^{(2)} = \frac{\sum_j \xi_{[j]} (\hat{\epsilon}_{[j]} \hat{\epsilon}_{[j]}^\top - \Upsilon_{[j]})}{\sum_j \xi_{[j]}} \quad \text{and} \quad \hat{\Phi}^{(4)} = \frac{\sum_j \xi_{[j]} \hat{\Phi}_{[j]}^{(4)}}{\sum_j \xi_{[j]}}$$

where $\hat{\epsilon}_{[j]} \equiv \hat{\theta}_{[j]} - \hat{\theta}_o$, $\xi_{[j]}$ is some weight, and $\hat{\Phi}_{[j]}^{(4)}$ is a d^4 -dimensional order 4 tensor such that

$$\begin{aligned} \hat{\Phi}_{[j], i_1, i_2, i_3, i_4}^{(4)} &\equiv \hat{\epsilon}_{[j], i_1} \hat{\epsilon}_{[j], i_2} \hat{\epsilon}_{[j], i_3} \hat{\epsilon}_{[j], i_4} + \Upsilon_{[j], i_1, i_2} \Upsilon_{[j], i_3, i_4} + \Upsilon_{[j], i_1, i_3} \Upsilon_{[j], i_2, i_4} + \Upsilon_{[j], i_1, i_4} \Upsilon_{[j], i_2, i_3} \\ &\quad - \Upsilon_{[j], i_1, i_2} \hat{\epsilon}_{[j], i_3} \hat{\epsilon}_{[j], i_4} - \Upsilon_{[j], i_1, i_3} \hat{\epsilon}_{[j], i_2} \hat{\epsilon}_{[j], i_4} - \Upsilon_{[j], i_1, i_4} \hat{\epsilon}_{[j], i_2} \hat{\epsilon}_{[j], i_3} \\ &\quad - \Upsilon_{[j], i_2, i_3} \hat{\epsilon}_{[j], i_1} \hat{\epsilon}_{[j], i_4} - \Upsilon_{[j], i_2, i_4} \hat{\epsilon}_{[j], i_1} \hat{\epsilon}_{[j], i_3} - \Upsilon_{[j], i_3, i_4} \hat{\epsilon}_{[j], i_1} \hat{\epsilon}_{[j], i_2}, \end{aligned}$$

where $\hat{\epsilon}_{[j], i}$ is the i -th component of the vector $\hat{\epsilon}_{[j]}$, and $\Upsilon_{[j], i_1, i_2}$ is the (i_1, i_2) element of the matrix $\Upsilon_{[j]}$.

A simple choice of $\xi_{[j]}$ is 1, motivated by the definition of $\Phi^{(2)}$ and $\Phi^{(4)}$ in Assumption 6.3. However, our preferred choice is $\xi_{[j]} = T_{[j]} \det(\hat{\Upsilon}_{[j]})^{-1/d}$ for the sake of efficiency as suggested by Armstrong et al. (2022); see Appendix A.2 therein.

7. Examples

In Section 7.1 we illustrate the proposed methods and check their statistical validity using simulated data. Then in Section 7.2 we analyze the effect of a mobility measure on the Covid-19 death data used in Bonvini et al. (2022). We assume that the observed data (deaths) are either Poisson or NB distributed, with means specified in Eq. (4). We focus on a single intervention, so that β_1 and A_t in Eq. (3) are scalars. Several model parameters are completely unidentifiable and need to be fixed. In particular, the maximum possible transmission rate was assumed to be $K = 6.5$, which is the largest value found in the literature (Liu et al., 2020). The generating distribution g and infection-to-death distribution π in Eq. (4) were assumed to be known and equal to those given in Bhatt et al. (2023); they are shown in Fig. 2. We also assumed that the ascertainment rate (the probability of death given infection) in Eq. (4) remained constant at $\alpha_t = 0.01$. The constant assumption is sensible here because the period was short and the number of susceptibles at the beginning of the epidemic was large. The specific value $\alpha_t = 0.01$

Table 1. *Coverage study results.* Coverages (%) of ML confidence and Bayesian credible intervals of β_1 for 5 different values of $\beta = (\beta_0, \beta_1)$ in Eq. (3) and seeding parameter $\mu = \log(100)$ in all cases. The priors for μ , β_0 and β_1 were hierarchical exponential, $N(0, 1/4)$ and shifted Gamma with mean 0.17 and variance 1/6, respectively, as in Bhatt et al. (2023).

β	(0, -2.2)	(0.25, -2.45)	(0.5, -2.7)	(0.75, -2.95)	(1, -3.2)
ML fit	93.2	95.5	93.7	96.1	95.0
Bhatt et al. (2023)	93.3	95.2	93.6	92.3	84.1

does not have to be accurate because it has no effect on the model parameters – any other value would yield the same estimates; it only has a multiplicative effect on the unknown latent infection values, which are not of primary interest here. Finally, we set $I_t = 0$ for $t \leq -T_0$ and $I_t = e^\mu$ for $t = -T_0 + 1, \dots, 0$, where μ is a parameter to be estimated and $T_0 = 40$, as described in Section 3 under ‘seeding values’.

7.1. Analyses of simulated datasets

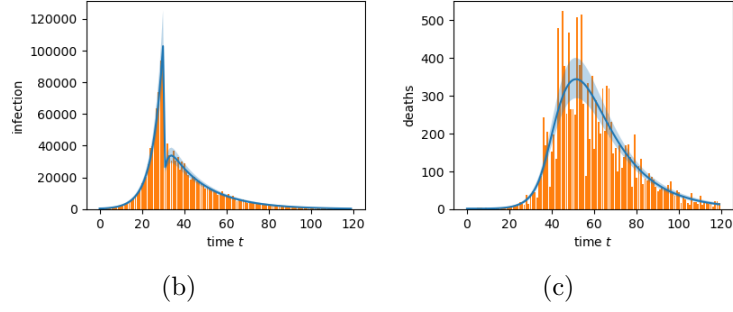
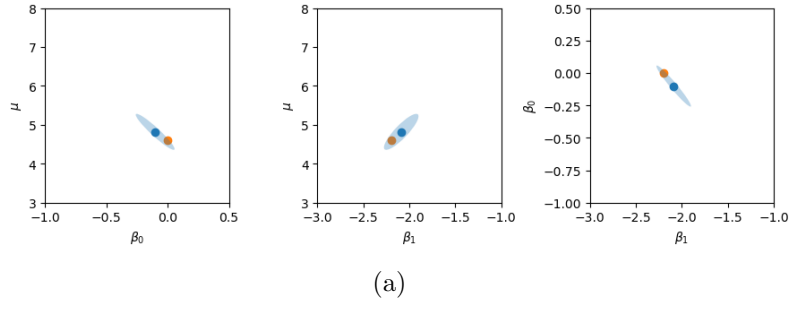
To illustrate that the algorithm in Appendix A yields sensible ML estimates, we simulated infection and death processes I_t and Y_t , $t = 1, \dots, 120$, from NB distributions (both I_t and Y_t are random variables) with means specified in Eq. (1) and “number of successes” parameters $r_I = 100$ for the infection process and $r_Y = 10$ for the death process, R_t in Eq. (3) with $(\mu, \beta_0, \beta_1) = (\log(100), 0, -2.2)$, and time-varying binary interventions $A_{1t} = 0$ for $t < 30$ and $A_{1t} = 1$ for $t \geq 30$. We fit the true mean model to the data by ML and using the Bayesian approach in Bhatt et al. (2023), assuming the correct NB model for the deaths Y_t but assuming that infections I_t were deterministic, since we cannot identify both the distributions of Y_t and I_t ; see Section 3. For the Bayesian approach, we used a shifted gamma prior with shape 1/6, scale 1 and shift $\log(1.05)/6$ for β_1 , corresponding to mean $(1 + \log(1.05))/6 = 0.17$ and variance 1/6, and a $N(0, 1/4)$ prior for β_0 . These choices match the model, priors, intervention values and parameter estimates in Bhatt et al. (2023), where they analyzed the effect of lockdown ($A_t = 1$) versus no lockdown ($A_t = 0$) on Covid cases in European countries. Finally, for μ we used the default prior in the Epidemia package: $e^\mu \sim \text{Exp}(e^{-\mu_0})$ with $e^{\mu_0} \sim \text{Exp}(\lambda)$ and $\lambda = 0.03$, so that μ has prior mean $\log(1/0.03) = 1.52$, which is close to the true value $\log(100) = 1.6$.

True parameters and simulated data are shown in orange in Fig. 3. Bayesian and ML estimates for (μ, β_0, β_1) and for the mean infection and death processes are overlaid in blue, together with confidence and credible intervals. All estimates appear reasonable and the confidence/credible intervals cover the true values, but with some notable differences between estimation methods. Appendix Fig. 12 shows that the Bayesian estimates and credible intervals can have poor properties when we use more informative priors. Next, we conduct a simulation study to evaluate the coverage of confidence and credible intervals.

Coverage of ML and Bayesian intervals Accurate inference about parameters is important not only to understand, for example, the effect of particular interventions, measured by β_1 , but also to produce accurate future predictions of the time course of epidemics, which is one main objective of epidemic models.

To evaluate the coverage of confidence and credible intervals, we set $(\mu, \beta_0, \beta_1) = (\log(100), 0, -2.2)$, simulated 1000 NB infection and death processes as above, fitted the NB model using both ML and Bayesian paradigms with priors as above, and recorded the proportion of times the confidence and credible intervals contained the true parameter. Table 1 contains the resulting empirical 95% coverages; other coverage values gave qualitatively similar results (not shown). We repeated the simulation for four other parameter values. The ML intervals have correct coverage up to simulation error in all cases, whereas the coverage of the Bayesian interval degrades when the prior means of β_0 and β_1 , 0 and 0.17 respectively, further deviate from the true

Maximum Likelihood Estimation



Bayesian Estimation

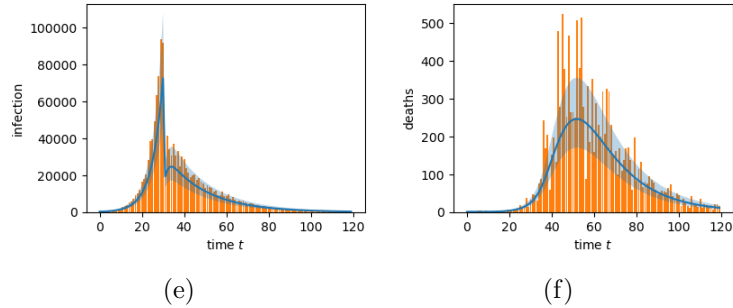
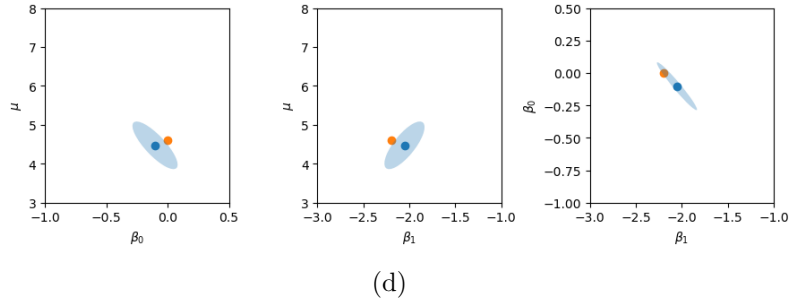


Fig. 3. True model parameters, simulated infections and deaths (orange), and overlaid ML and Bayesian estimates (blue), together with 95% confidence/credible intervals (light blue). The infection process in (b,e) and death process in (c,f) were simulated from NB distributions with means in Eq. (1), R_t in Eq. (3), true parameters $\mu = \log(100)$, $\beta_0 = 0$ and $\beta_1 = -2.2$ in (a,d), and binary intervention process $M_t = 0$ for $t < 30$ and $M_t = 1$ for $t \geq 30$. The model in Eqs. (3) and (4) was fitted assuming NB deaths.

values. Note that it is not easy to choose a prior without additional information, as illustrated in Fig. 13, which shows simulated death processes when $(\mu, \beta_0, \beta_1) = (\log(100), 0, -2.2)$ and $(\mu, \beta_0, \beta_1) = (\log(25), 1, -3.2)$: all simulated data look very similar and we would be hard pressed

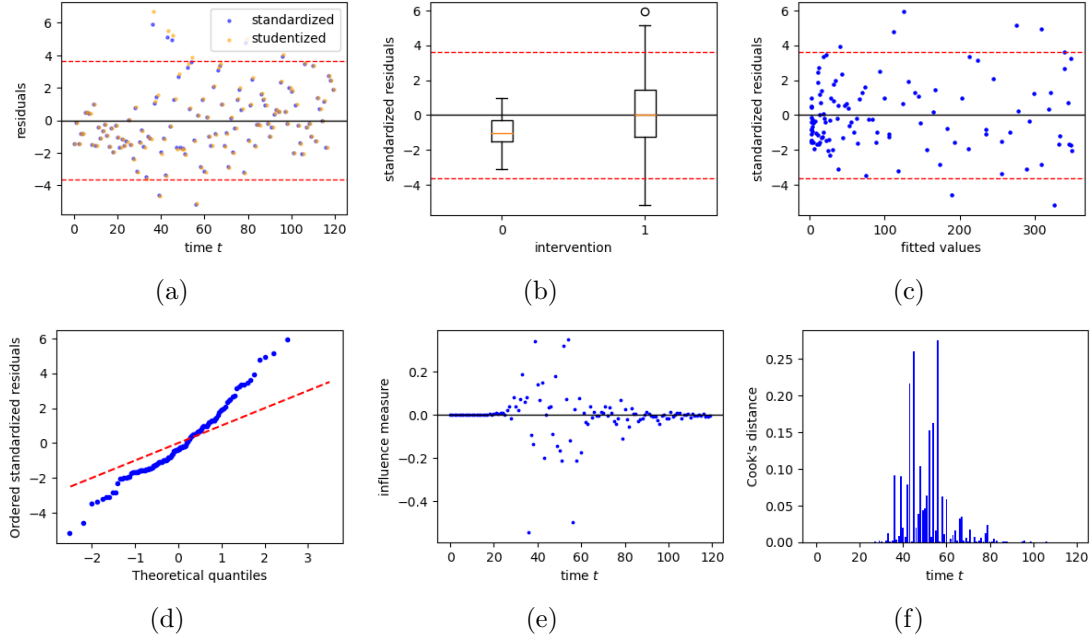


Fig. 4. Diagnostics for the Gaussian model fitted to the NB data shown in Fig. 3. (a) Standardized and studentized residuals versus t . (b) Standardized residuals versus A_t and (c) versus \hat{Y}_t . (d) QQ plot of standardized residuals. (e) Influence on $\hat{\beta}_1$ and (f) Cook's distance, versus t . Panels (b) and (d) suggest that the Gaussian distribution is not a good choice to model the variance of Y_t .

to pick different priors for them. It would therefore be wise to select priors that are not too informative.

Model checking Bayesian and ML approaches provide the alternative option of fitting a Gaussian model to the data. Here we illustrate that the standard diagnostics derived from an ML fit can detect model inadequacies; see Section 4. Appendix C Fig. 15 shows these diagnostics for the NB model fitted by ML to the simulated NB data shown in Fig. 3. As expected, all diagnostics look fine, since we fit the correct model (except that the model assumes that the latent infection process is deterministic). Appendix C Fig. 14 shows the Gaussian model fitted to the same data, and Fig. 4 shows the corresponding diagnostics, where it is clear particularly from panels (b) and (d) that the Gaussian distribution is not a good choice to model the variance of Y_t . (When model diagnostics fail, as is the case in Fig. 4, case diagnostics in (e,f) can look pathological even if there are no outliers or influential observations, so it is best to avoid over-interpreting them.)

Empirical Bayes Analysis Suppose now that we have data from $N = 100$ different geographic regions with corresponding parameters $\theta_i = (\mu_i, \beta_{0i}, \beta_{1i})$, i, \dots, N . We estimate the θ_i 's by maximum likelihood, and take advantage of similarities between the parameters by shrinking the individual estimates towards each other, as described in Section 6. We now evaluate by simulation the coverage of the resulting confidence intervals, for the three scenarios depicted in Fig. 5:

- (a) (μ, β_0, β_1) are independent Gaussian random vectors with mean $(\log(300), 0, -2)$ and covariance diagonal $(0.5, 0.3, 0.3)$.
- (b) (β_0, β_1) are Gaussian vectors with mean $(0, -2)$ and covariance $\begin{pmatrix} 0.3 & -0.28 \\ -0.28 & 0.3 \end{pmatrix}$; μ is independent of (β_0, β_1) and normally distributed with mean $\log(300)$ and variance 0.5.

Table 2. *Shrinkage study result.* Coverages (%) of ML confidence and Bayesian credible intervals for the three sets of parameters shown in Fig. 5.

Scenario	(a)	(b)	(c)
ML fit	92	98	95
Bhatt et al. (2023)	91	62	34

(c) (μ, β_0, β_1) have a mixture distribution with two equal Gaussian components with means $(\log(150), 0.5, -2.5)$ and $(\log(600), -0.5, -1.5)$, and covariance matrix $\begin{pmatrix} 1 & 0 & 0 \\ 0 & 0.5 & -0.25 \\ 0 & -0.25 & 0.5 \end{pmatrix}$ for both components.

The settings in (a), (b) and (c) were chosen so that the marginal means and variances of μ , β_0 and β_1 would be the same, as well as the covariances of (β_0, β_1) in (b) and (c). These choices allowed us to use the same priors in the three scenarios, so coverage differences could not be attributed to difference in priors. We used the hierarchical model of Bhatt et al. (2023):

$$\begin{aligned} e^{\mu_i} &\sim \text{Expon}(e^{-\mu^*}), \\ \beta_{0i} &\sim N(\beta_0^*, \sigma_0^2), \\ \beta_{1i} &\sim N(\beta_1^*, \sigma_1^2), \end{aligned} \tag{11}$$

where $(\mu^*, \beta_0^*, \beta_1^*)$ and $(\mu_i, \beta_{0i}, \beta_{1i})$ denote the global and regional parameters, respectively, with priors and hyper-priors

$$\begin{aligned} e^{\mu^*} &\sim \text{Expon}(0.03), \\ \beta_0^* &\sim N(0, 1/4), & \sigma_0 &\sim \text{Gamma}(2, 0.25), \\ \beta_1^* &\sim -\log(1.05)/6 - \text{Gamma}(1/6, 1), & \sigma_1 &\sim \text{Gamma}(0.5, 0.25). \end{aligned} \tag{12}$$

Fig. 5 shows $N = 100$ simulated (β_0, β_1) in each scenario, Fig. 6 shows their shrunk ML estimates together with 95% confidence intervals, Fig. 7 shows the corresponding Bayesian estimates, and Table 2 contains the proportion of intervals that contain the true values of (μ, β_0, β_1) . Point and interval estimates are strikingly different across methods, the ML estimates being much closer to the true values. The coverage of the credible intervals also degrades badly as the true dependence structure of the $(\mu_i, \beta_{0i}, \beta_{1i})$ deviates from their assumed independent prior distributions in Eqs. (11) and (12). One could presumably obtain better Bayesian coverage with better priors, although they would be hard to design a priori. On the other hand, ML estimation yields the correct coverage in all cases, up to random error.

7.2. Analysis of Covid-19 time series of deaths in the United States

We analyzed the effect of a mobility measure on the Covid-19 death data in US states used in Bonvini et al. (2022). The data are from the Delphi repository at Carnegie Mellon University `delphi.cmu.edu`. The data consist of daily observations, at the state level, on the number of Covid-19 deaths Y_t (Fig. 8) and a measure of mobility “proportion of full-time work”, A_t , (Fig. 17(a)), which is the fraction of mobile devices that spent more than 6 hours at a location other than their home during the daytime (SafeGraph’s `full_time_work_prop`). In all states, mobility varied approximately from 5% to 11%, depending on week day, up to mid-March 2020, when mobility dropped to about 3.5% with much less variability across weekdays, and slowly climbed back up to about 4.5% by August 2020. The time period considered in the analysis was February 15 2020 to August 1 2020 (168 days). We focused on the 30 states that reported

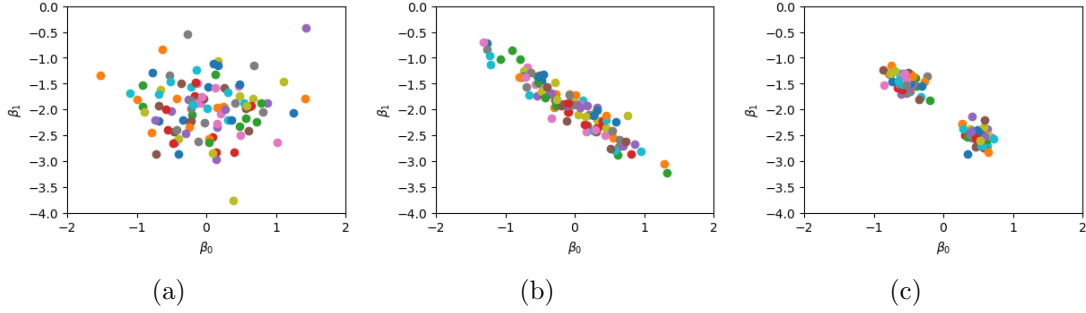


Fig. 5. Simultaneous estimation at $N = 100$ locations. True β 's simulated in three scenarios.

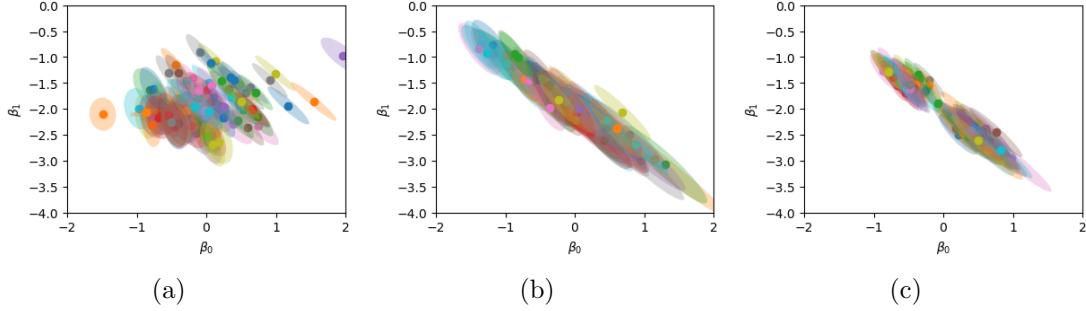


Fig. 6. Shrunken ML estimates of $\hat{\beta}$ and confidence intervals for the true β 's in Fig. 5.

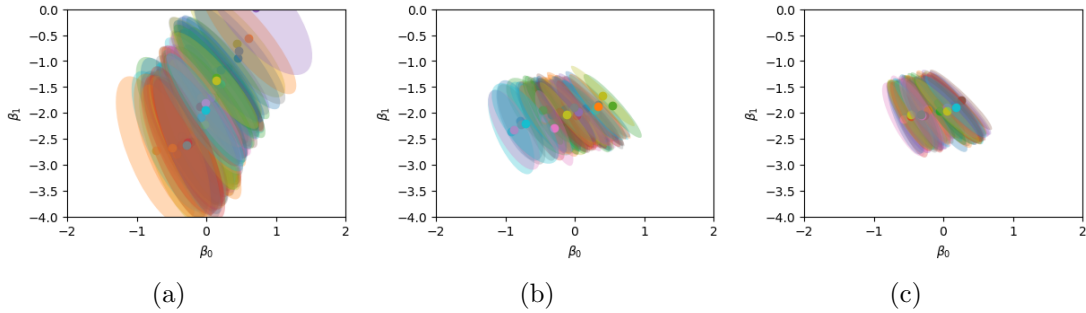


Fig. 7. Bayesian estimates and credible intervals for the true β 's in Fig. 5, using Bhatt et al. (2023).

over 20 deaths on one or more days at least one day, and we truncated the time series 30 days prior to 10 accumulated deaths, as in Bhatt et al. (2023). This shaved 10 days of data at the start of the period, leaving 158 days of data in each state for analysis, from February 25 to August 1. The death time series showed a strong weekend effect: fewer deaths were reported on Saturdays and Sundays than one would expect from the numbers reported the previous weeks, and these deaths were instead reported mostly on the following Mondays, and Tuesdays and Wednesdays. Because this effect is not accounted for by the model, it adds variability to the analysis that is due to the reporting process rather than to the epidemic process. For that reason, we pre-processed the data to reduce the effect: for each state, we fitted a nonparametric smooth function to the data together with four additional parameters that estimated the excess Monday, Tuesday and Wednesday effects and deficit saturday effect; we subtracted the estimated effects from all corresponding days and added their sum to all Sundays. Fig. 16 shows the original and adjusted data for four states.

Fig. 8 displays the ML mean death fits for the 30 states, assuming NB death data and regression mean specified in Eqs. (3) and (4). While the overall profiles of the fitted means appear reasonable in all states, in several states there are obvious mismatches between observed

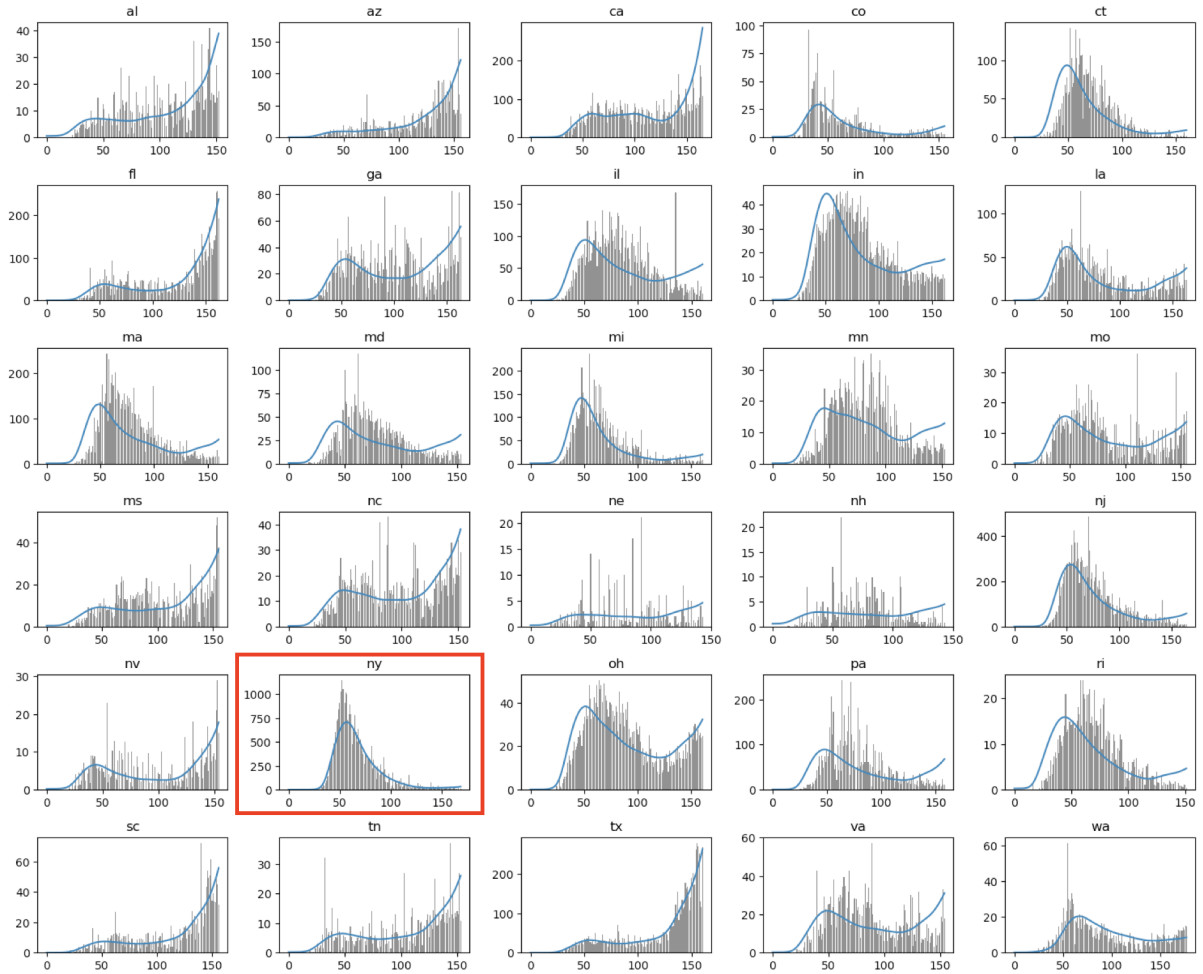


Fig. 8. ML fits (blue) to Covid-19 deaths times series in 30 US states from Feb 15 (day 1) to August 1st (day 158) 2020 period . New York is indicated with a box.

and fitted onsets of the pandemic. A possible explanation for this mismatch is a mis-specified infection-to-death distribution π in Fig. 2; perhaps π should be state specific to account for differences between states, such as different delays in reporting deaths.

Fig. 9 shows model and case diagnostics for the ML fit in NY state. In Fig. 8, there is no apparent onset mismatch in that state but the diagnostics in Fig. 9(a) clearly shows lack of fit at the start and very end of the epidemic, where residuals are not random. A more flexible model for R_t is needed. The other plots don't point to additional issues other than two outliers in (a), only one of which, at $t = 140$, has a very modest influence on the fit: the ML estimates of (μ, β_0, β_1) are $(2.08, -7.66, 14.74)$ and $(2.02, -7.82, 15.14)$ with and without that point; the fitted R_t and mean death process with and without that point are shown in Appendix Fig. 18. Finally, the seemingly influential points at the end of the range in Fig. 9(e) are due model lack of fit and are not otherwise suspicious. We also checked the model adequacy in the other states (not shown): apart from the obvious onset mismatches pointed out above, the model and case diagnostics did not raise much concerns.

Fig. 10(a) displays the ML estimates of β_1 for the 30 states, fitted separately and together using the empirical Bayes shrinkage method in Section 6. Fig. 10(b) displays the Bayesian estimates fitted separately and together, as in Bhatt et al. (2023). Note that we scaled and shifted A_t so that the values would be mostly in the $[0, 1]$ range, to match the binary interventions in

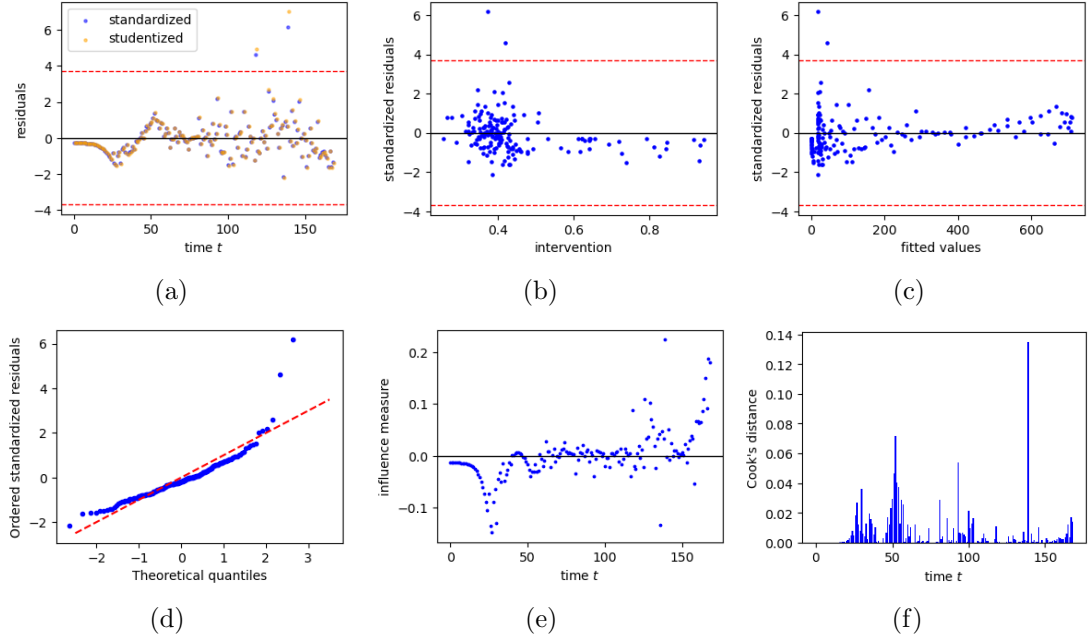


Fig. 9. Model diagnostic plots for NY. (a) Standardized and studentized residuals versus t . (b) Standardized residuals versus A_t and (c) versus \hat{Y}_t . The red dashed lines are the $\alpha/2n$ quantiles of the Gaussian distribution. (d) QQ plot of standardized residuals. (e) Specific influence on $\hat{\beta}_1$ and (f) Cook's distance versus t .

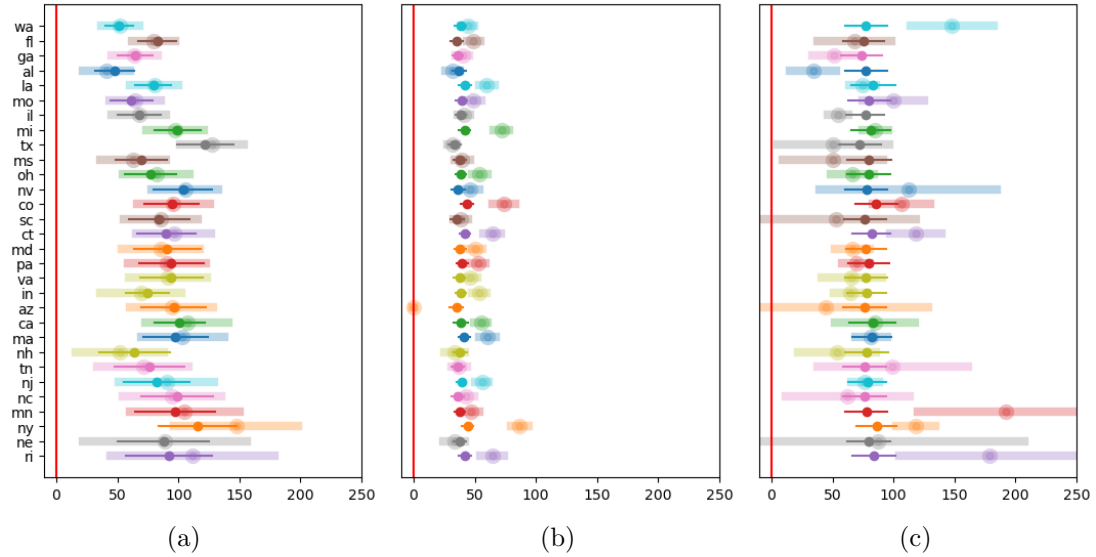


Fig. 10. Estimates and confidence intervals for β_1 in Eq. (3) for 30 states using (a) ML and robust empirical Bayes, (b) Bhatt et al. (2023) with their priors and (c) with less informative priors. The faint thick lines are the estimates and intervals before shrinkage and the dark thin lines after shrinkage. The 30 states are sorted along the y-axis by increasing order of $\text{Var}(\hat{\beta}_1)$ before shrinkage.

Bhatt et al. (2023), so we could use their prior distributions; see Fig. 17. However, the estimates of β_1 in Fig. 10 are displayed on the original scale. The two estimation methods in Figs. 10(a) and 10(b) produce strikingly different inferences: the Bayesian estimates of β_1 take values in a narrow range around 50 and they have very narrow credible intervals, while the ML estimates have a much larger spread around 100 and their confidence intervals are wider. Clearly, the priors are inappropriate for this data; they are centered on the wrong values and their variances

are too small. Fig. 10(c) shows the Bayesian estimates using less informative priors, specifically Eq. (11) with hyper-priors[†]

$$\begin{aligned} e^{\mu^*} &\sim \text{Expon}(0.03), \\ \beta_0^* &\sim N(0, 4), & \sigma_0 &\sim \text{Gamma}(1, 8), \\ \beta_1^* &\sim N(0, 4), & \sigma_1 &\sim \text{Gamma}(1, 8). \end{aligned}$$

Now most Bayesian estimates of β_1 take values around 100, which is reassuring since they are closer to the ML estimates. But, ultimately, we have more confidence in the ML estimates given the simulation results in Table 2. Note also that, in some states, the shrunk Bayesian estimates are drastically different from the marginal Bayesian estimates, and the credible intervals for the shrunk estimates are rather narrow compared to their un-shrunk counterparts, which may point to some deficiencies of the Bayesian hierarchical model.

Because the logistic function in Eq. (3) is non-linear, estimates of β_1 are useful for comparing qualitatively the effect of mobility across states – e.g. decreasing mobility has a large effect in NY and TX and a small effect in AL and WA in Fig. 10 – but their specific values are not particularly interpretable. Changes in R_t are more meaningful; for example, Fig. 18 shows that in NY state, R_t decreased from 6 to just below 1 when mobility dropped suddenly mid-March 2020. This drop is in the same ballpark as the drops observed in European countries when government mandated mobility interventions were implemented (Scott et al., 2021).

Lastly, Fig. 11 shows future death predictions and prediction intervals (Section 5) for NY state under two hypothetical trajectory mobility A_t , based on the shrunk estimates. The Bayesian and ML predictions are strikingly different. We have much more confidence in the latter, although we do not have perfect confidence since the model exhibits some lack of fit, as evidenced in Fig. 9.

8. Discussion

We have discussed statistical inference for a semi-mechanistic epidemic model using frequentist methods. The advantage of using frequentist methods is that there is no need to specify prior distributions and the confidence intervals have valid coverage properties. However, the disadvantage is that these coverage properties are asymptotic in nature in the sense that they hold as the total number of time points T increases.

If the user has informative priors that they want to include then it is possible to do so while preserving frequentist coverage. For example, inverting a test based on the integrated likelihood allows one to include a prior and still have frequentist coverage.

We made simplifying assumptions that are not always reasonable. We assumed $\alpha_t = \alpha_0$, meaning that the probability that an infected individual produces an outcome (e.g. dies) remains constant over time, which is not reasonable unless the time series are short enough that nothing in the environment changes. Otherwise, changes in virus mutation, medical treatment, season, etc. will affect α_t . The same argument applies to R_t . Our model does allow R_t to vary with t through A_t but a more elaborate model would allow K to also vary with t since, for example, not all variants are as deadly, and part of the population will become immune for a while. One could also use a more flexible model for R_t , for example by replacing A_t with a spline basis evaluated at A_t . Another improvement would be to let π vary by location. Furthermore, one could let g vary with time. All of these generalizations are possible in principle but one has to balance with desire for more complex (and realistic) models with the fact that there is limited information. Informative priors can help but at the cost of losing frequentist coverage properties which is one of the goals of this paper.

[†]For full disclosure, we originally used $N(0, 8)$ for β_0^* and β_1^* , which gave estimates of β_1 around 600; these were too different from the MLEs for comfort. We suspect that overly uninformative hyper priors yielded improper posteriors. We subsequently tweaked the hyper priors so that the shrunk Bayesian estimates would be closer to the MLEs.

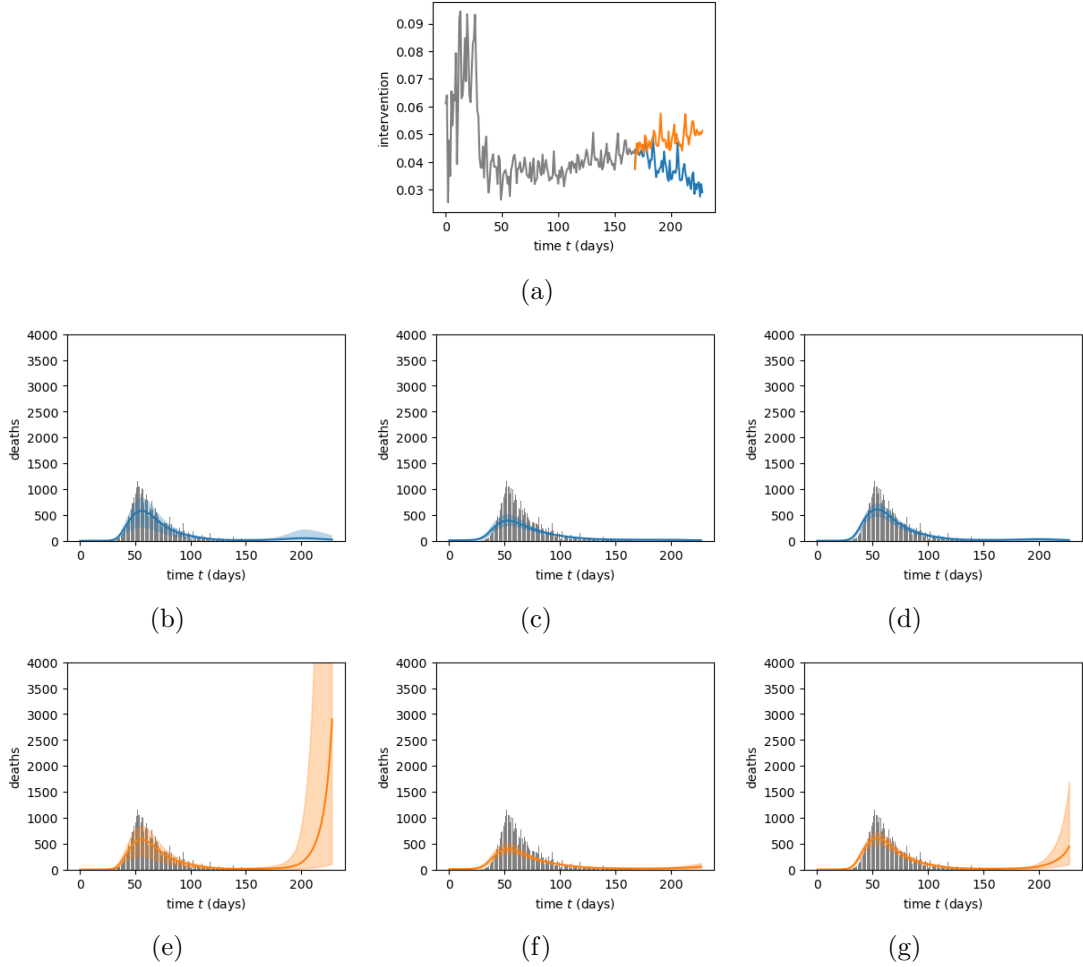


Fig. 11. Counterfactual predictions for NY state. (a) Observed intervention ($t \leq 168$) and two future scenarios ($t > 168$) in blue and orange. (b,e) Counterfactual mean deaths $\mathbb{E}[Y_t]$ with 95% global confidence bands based on the ML shrinkage estimator (Section 6). (c,f) Corresponding Bayesian predictions using the informative priors in Eqs. (11) and (12), and (d,g) using the less informative priors.

The code for the methods in this paper is freely available in our Python package `freqepid`. Code vignettes we used to generate the results in Section 7 are available at github.com/HeejongBong/freqepid. Inspiration for this project came from the R package `Epidemia`. Currently, that package implements a wider range of models compared to `freqepid` but, in principle, the methods there can be extended to provide the same utility as `Epidemia`. We have found that the models in `freqepid` often work well even if the generating processes do not match the model.

Acknowledgement

The authors thanks the Delphi group (delphi.cmu.edu) for providing funding the first author on this project.

References

Armstrong, T. B., Kolesár, M., and Plagborg-Møller, M. (2022). Robust empirical bayes confidence intervals. *Econometrica*, 90(6):2567–2602.

- Baker, R. E., Park, S. W., Yang, W., Vecchi, G. A., Metcalf, C. J. E., and Grenfell, B. T. (2020). The impact of covid-19 nonpharmaceutical interventions on the future dynamics of endemic infections. *Proceedings of the National Academy of Sciences*, 117(48):30547–30553.
- Bates, S., Kennedy, E., Tibshirani, R., Ventura, V., and Wasserman, L. (2022). Causal inference with orthogonalized regression: Taming the phantom. *arXiv preprint arXiv:2201.13451*.
- Bhatt, S., Ferguson, N., Flaxman, S., Gandy, A., Mishra, S., and Scott, J. A. (2023). Semi-mechanistic bayesian modelling of covid-19 with renewal processes. *Journal of the Royal Statistical Society Series A: Statistics in Society*, 186(4):601–615.
- Bong, H., Ventura, V., and Wasserman, L. (2023). Contribution to the discussion of ‘the second discussion meeting on statistical aspects of the covid-19 pandemic’. *Journal of the Royal Statistical Society Series A: Statistics in Society*, 186(4):645–646.
- Bonvini, M., Kennedy, E. H., Ventura, V., and Wasserman, L. (2022). Causal inference for the effect of mobility on COVID-19 deaths. *The Annals of Applied Statistics*, 16(4):2458 – 2480.
- Chatzilena, A., van Leeuwen, E., Ratmann, O., Baguelin, M., and Demiris, N. (2019). Contemporary statistical inference for infectious disease models using stan. *Epidemics*, 29:100367.
- Fintzi, J., Wakefield, J., and Minin, V. N. (2022). A linear noise approximation for stochastic epidemic models fit to partially observed incidence counts. *Biometrics*, 78(4):1530–1541.
- Giacomini, R. and Kitagawa, T. (2021). Robust bayesian inference for set-identified models. *Econometrica*, 89(4):1519–1556.
- Gunaratne, C., Reyes, R., Hemberg, E., and O’Reilly, U.-M. (2022). Evaluating efficacy of indoor non-pharmaceutical interventions against covid-19 outbreaks with a coupled spatial-sir agent-based simulation framework. *Scientific reports*, 12(1):1–11.
- Gustafson, P. (2015). *Bayesian inference for partially identified models: Exploring the limits of limited data*, volume 140. CRC Press.
- James, W. and Stein, C. (1960). Estimation with quadratic loss. In *Proceedings of the Fourth Berkeley Symposium on Mathematical Statistics and Probability*, volume 1, page 361. Univ of California Press.
- Kermack, W. O., McKendrick, A., and Walker, G. T. (1927). A contribution to the mathematical theory of epidemics. *Proceedings of the Royal Society of London. Series A, Containing Papers of a Mathematical and Physical Character*, 115:700–721.
- Lazebnik, T., Shami, L., and Bunimovich-Mendrazitsky, S. (2022). Spatio-temporal influence of non-pharmaceutical interventions policies on pandemic dynamics and the economy: the case of covid-19. *Economic Research-Ekonomska Istraživanja*, 35(1):1833–1861.
- Li, Y. I., Turk, G., Rohrbach, P. B., Pietzonka, P., Kappler, J., Singh, R., Dolezal, J., Ekeh, T., Kikuchi, L., Peterson, J. D., et al. (2021). Efficient bayesian inference of fully stochastic epidemiological models with applications to covid-19. *Royal Society Open Science*, 8(8):211065.
- Liu, Y., Gayle, A. A., Wilder-Smith, A., and Rocklöv, J. (2020). The reproductive number of covid-19 is higher compared to sars coronavirus. *Journal of travel medicine*.
- Morris, C. N. (1983). Parametric empirical bayes inference: theory and applications. *Journal of the American statistical Association*, 78(381):47–55.
- Newey, W. K., West, K. D., et al. (1987). A simple, positive semi-definite, heteroskedasticity and autocorrelation consistent covariance matrix. *Econometrica*, 55(3):703–708.

- Perra, N. (2021). Non-pharmaceutical interventions during the covid-19 pandemic: A review. *Physics Reports*, 913:1–52.
- Pötscher, B. M. and Prucha, I. R. (1997). *Dynamic Nonlinear Econometric Models: Asymptotic Theory*. Springer, Berlin, Heidelberg.
- Robins, J. M. and Wasserman, L. A. (1997). Estimation of effects of sequential treatments by reparameterizing directed acyclic graphs. *Proceedings of the Thirteenth Conference on Uncertainty in Artificial Intelligence, Providence Rhode Island*.
- Scott, J. A., Gandy, A., Mishra, S., Bhatt, S., Flaxman, S., Unwin, H. J. T., and Ish-Horowicz, J. (2021). Epidemia: an r package for semi-mechanistic bayesian modelling of infectious diseases using point processes. *arXiv preprint arXiv:2110.12461*.
- Smith, J. E. (1995). Generalized chebychev inequalities: theory and applications in decision analysis. *Operations Research*, 43(5):807–825.
- van der Vaart, A. W. (2000). *Asymptotic statistics*, volume 3. Cambridge university press.
- Vytla, V., Ramakuri, S. K., Peddi, A., Srinivas, K. K., and Ragav, N. N. (2021). Mathematical models for predicting covid-19 pandemic: a review. In *Journal of Physics: Conference Series*, volume 1797, page 012009. IOP Publishing.

A. Appendix: Block Coordinate Descent Algorithm

In the main paper, A_t denotes a vector of interventions. For notation brevity, in all the appendices we will append 1 at the start of A_t so that the expression $\beta_0 + \beta_1^\top A_t$ in the main text can simply be written $\beta^\top A_t$ in the proofs.

Given observed data \bar{Y}_T , we fit our model, (Eq. (4)) by maximizing the log likelihood function

$$\ell(\theta) \equiv \sum_{t=1}^T \log p(Y_t; \theta) = \sum_{t=1}^T \ell_t(\theta).$$

Because the MLE for θ is not in a closed form, we use the coordinate descent algorithm to find the maximizer. For the first iteration, let $\hat{\beta}^{(0)}$ and $\hat{\mu}^{(0)}$ be the starting values given below. For iteration $i > 1$, let $\hat{\beta}^{(i-1)}$ and $\hat{\mu}^{(i-1)}$ be the outcomes of the previous iteration. We set $\hat{\nu}^{(i)}$ by the maximizer of the likelihood function given β and μ are fixed at $\hat{\beta}^{(i-1)}$ and $\hat{\mu}^{(i-1)}$. For the Normal distribution, the maximizer has a closed form:

$$\hat{\nu}^{(i)} = \frac{1}{\sqrt{T}} \|\bar{Y}_T - \hat{\mu}^{(i-1)}(\Pi\Omega(\hat{\beta}^{(i)}) + \Pi_0)\mathbf{1}\|_2. \quad (13)$$

For the NB distribution, the maximizer $\hat{\nu}^{(i)}$ is obtained by numerically solving

$$\hat{\nu}^{(i)} = \arg \min_{\nu} \ell(\nu, \hat{\mu}^{(i-1)}, \hat{\beta}^{(i-1)}).$$

Next, we use Newton’s method to perform a coordinate descent step for β and μ . The steps are:

$$(\hat{\beta}^{(i)}, \hat{\mu}^{(i)}) = (\hat{\beta}^{(i-1)}, \hat{\mu}^{(i-1)}) + \eta [\nabla_{(\beta, \mu)}^2 \ell(\hat{\beta}^{(i-1)}, \hat{\mu}^{(i-1)}, \hat{\nu}^{(i)})]^{-1} \nabla_{(\beta, \mu)} \ell(\hat{\beta}^{(i-1)}, \hat{\mu}^{(i-1)}, \hat{\nu}^{(i)})$$

where $\ell(\beta, \mu, \nu)$ is the log-likelihood function given data \bar{Y}_T , and η is a step size hyperparameter. We iterate the algorithm until the log-likelihood converges at a threshold hyperparameter.

Starting Values The coordinate descent algorithm and Newton's method require starting values $\hat{\beta}^{(0)}$ and $\hat{\mu}^{(0)}$. Our approach is as follows. Start by approximating π with a point mass at its mean $\bar{\pi}$ so that $Y_t = \alpha I_{t-\bar{\pi}}$. Then an initial estimate of \bar{I}_0 is $(Y_{-k+\bar{\pi}+1}/\alpha, \dots, Y_{\bar{\pi}}/\alpha)$. We obtain $\hat{\mu}^{(0)} = \log(\frac{1}{\alpha k} \sum_{t=-k+\bar{\pi}+1}^{\bar{\pi}} Y_t)$. We then have from Eq. (3)

$$Y_{t+\bar{\pi}} = K(1 + e^{-\beta^\top A_t})^{-1} \sum_{s < t} Y_{s+\bar{\pi}} g_{t-s}.$$

Now approximate $(1 + e^{-\beta^\top A_t})^{-1} \approx \frac{1}{2} + \frac{1}{4}\beta^\top A_t$. This leads to the linear regression

$$Y_{t+\bar{\pi}} = \frac{1}{2}K \sum_{s < t} Y_{s+\bar{\pi}} g_{t-s} + \frac{1}{4}K\beta^\top A_t \sum_{s < t} Y_{s+\bar{\pi}} g_{t-s},$$

and we obtain the least square estimates $\hat{\beta}^{(0)}$. We note that the starting value for ν is not required for the estimation algorithm.

B. Appendix: Proofs

Proof of Proposition 3.1 Conditional on \bar{I}_T , the Y_t 's are mutually independent and $\bar{I}_T \equiv \bar{I}_T(\beta, \mu)$ is deterministic given parameters β and μ . Hence, the conditional distribution of Y_t given \bar{A}_t is equal to the conditional distribution of Y_t given $(\bar{I}_t, \bar{Y}_{t-1}, \bar{A}_t)$ (and hence given $(\bar{I}_t, \bar{Y}_{t-1})$), which we take to be Gaussian or NB with nuisance parameter ν and mean $m_t(\beta, \mu) \equiv \mathbb{E}_\theta[Y_t | \bar{A}_t]$, where \mathbb{E}_θ denotes the expectation under model (4) with parameter θ . Because $\bar{I}_0 = e^\mu \mathbf{1}$, $m_1(\beta, \mu)$ is given by $\alpha e^\mu \sum_{t=1}^{T_0} \pi_t$, and because $\alpha \sum_{s=1}^{T_0} \pi_t > 0$, μ is identified by the marginal mean of Y_1 , that is $\mu = \log\left(\frac{\mathbb{E}_\theta[Y_1 | \bar{A}_1]}{\alpha \sum_{s=1}^{T_0} \pi_t}\right)$. Similarly, because ν is an identified parameter of the Gaussian and NB distributions, it is identified by the marginal distribution of Y_1 .

Now it is sufficient to show that β is identified given that μ and ν are fixed. We proceed with a proof by contradiction. Suppose that the marginal means of \bar{Y}_T under β and β' are the same, that is $\bar{m}_T(\beta, \mu) = \bar{m}_T(\beta', \mu)$. This implies that $\bar{I}_{T-T_0}(\beta, \mu) = \bar{I}_{T-T_0}(\beta', \mu)$. To prove this, suppose that $\exists t \in \{2, \dots, T-T_0\}$ such that $\bar{I}_{t-1}(\beta, \mu) = \bar{I}_{t-1}(\beta', \mu)$ and $I_t(\beta, \mu) \neq I_t(\beta', \mu)$. Defining $\tau \equiv \min\{t : g_t > 0\}$, we have $\tau \leq T_0$, and

$$m_{t+\tau}(\beta, \mu) = \alpha \sum_{s=0}^{t+T_0-1} \pi_{s+\tau} I_{t-s}(\beta, \mu).$$

Because $\bar{I}_{t-1}(\beta, \mu) = \bar{I}_{t-1}(\beta', \mu)$, $\sum_{s=1}^{t+T_0-1} \pi_{s+\tau} I_{t-s}(\beta, \mu) = \sum_{s=1}^{t+T_0-1} \pi_{s+\tau} I_{t-s}(\beta', \mu)$. As a result, $m_{t+\tau}(\beta, \mu) = m_{t+\tau}(\beta', \mu)$ implies that $I_t(\beta, \mu) = I_t(\beta', \mu)$. This contradicts our premise that $\bar{I}_{T-T_0}(\beta, \mu) \neq \bar{I}_{T-T_0}(\beta', \mu)$. The identity in infection \bar{I}_{T-T_0} implies $\bar{R}_{T-T_0}(\beta) = \bar{R}_{T-T_0}(\beta')$. In other words, $(\beta - \beta')A_t = 0$ for all $t \leq T - T_0$, from which we conclude that $\beta = \beta'$.

B.1. Lemmas and Proofs for Section 5

We need the following lemma for the proof of Theorem 5.7.

LEMMA B.1. *Suppose that Assumption 5.4 holds. For the NB distribution, we further assume that $r_{\min} > 1$. Then Θ as defined in Definition 5.5 is a compact set with probability 1. Moreover, there exist $\mathfrak{F}(\bar{A}_T)$ -measurable random variables $R_{\min}, R_{\max}, \nu_{\min}, \nu_{\max} > 0$ such that, for any $t \geq 1$*

$$(\beta, \mu, \nu) \in \Theta \implies R_{\min} \leq R(\bar{A}_t, \beta) \leq R_{\max} \text{ and } \nu_{\min} \leq \nu \leq \nu_{\max},$$

with probability 1.

PROOF. For $t \geq \tau$, $\mathbb{E}_\theta[I_t|\bar{A}_t] = R(\bar{A}_t, \beta) \sum_{s=1}^{\tau-1} \pi_s I_{t-s}$. Because $I_{\min} \leq I_{t-s} \leq I_{\max}$ for $s \in \{0, \dots, \tau-1\}$,

$$R(\bar{A}_t, \beta)I_{\min} \leq \mathbb{E}_\theta[I_t|\bar{A}_t] = I_t \leq I_{\max}.$$

This implies for $t \geq \tau$, $R(\bar{A}_t, \beta) \leq \frac{I_{\max}}{I_{\min}}$ and similarly $R(\bar{A}_t, \beta) \geq \frac{I_{\min}}{I_{\max}}$. According to Eq. (3), there exists $M > 0$ such that $\frac{I_{\min}}{I_{\max}} \leq R(\bar{A}_t, \beta) \leq \frac{I_{\max}}{I_{\min}} \implies |\beta^\top A_t| < M$. As a result, $\|\beta\|_2^2 \leq \frac{1}{\lambda_{\min, A} (T-\tau)} \|\beta^\top (A_{\tau+1}, \dots, A_T)\|_2^2 \leq \frac{M^2}{\lambda_{\min, A}}$. Moreover, $|\beta^\top A_t| \leq \|\beta\|_2 \|A_t\|_2 \leq \frac{MA_{\max}}{\sqrt{\lambda_{\min, A}}}$, which implies by Eq. (3) that $R_{\min} \leq R(\bar{A}_t, \beta) \leq R_{\max}$ for any $t \geq 1$, where R_{\min} and R_{\max} are constants depending on M , $\lambda_{\min, A}$ and A_{\max} .

Next, according to Eq. (4),

$$R_{\min} e^\mu \sum_{t=1}^{T_0} \pi_t \leq \mathbb{E}_\theta[I_1|\bar{A}_1] = R(\bar{A}_1, \beta) e^\mu \sum_{t=1}^{T_0} \pi_t \leq R_{\max} e^\mu \sum_{t=1}^{T_0} \pi_t.$$

Because $I_{\min} \leq \mathbb{E}_\theta[I_1|\bar{A}_1] \leq I_{\max}$, μ is bounded by

$$\log \left(\frac{I_{\min}}{R_{\max} \sum_{t=1}^{T_0} \pi_t} \right) \leq \mu \leq \log \left(\frac{I_{\max}}{R_{\min} \sum_{t=1}^{T_0} \pi_t} \right).$$

Finally, for the Normal distribution, $r_{\min} \leq \frac{T\nu^2}{\sum_t \mathbb{E}_\theta[Y_t|\bar{A}_t]} \leq r_{\max}$. Because

$$\min\{e^\mu, I_{\min}\} \sum_{t=1}^{T_0} \pi_t \leq \mathbb{E}_\theta[Y_t|\bar{A}_t] \leq e^\mu + I_{\max},$$

ν is bounded away from 0 and ∞ . For the NB distribution,

$$r_{\min} \leq 1 + \frac{1}{\nu} \frac{\sum_t \mathbb{E}_\theta[Y_t|\bar{A}_t]^2}{\sum_t \mathbb{E}_\theta[Y_t|\bar{A}_t]} \leq r_{\max}.$$

Because $r_{\min} > 1$, ν is again bounded away from 0 and ∞ . In sum, Θ is bounded almost surely.

Furthermore, the functions

$$(\beta, \mu) \mapsto \mathbb{E}_\theta[I_t|\bar{A}_t] \text{ and } \theta \mapsto \text{Var}_\theta[Y_t|\bar{A}_t]$$

are continuous. As an intersection of the preimages of closed sets by the three continuous functions, Θ is closed almost surely. It follows that Θ is compact almost surely. \square

Proof of Theorem 5.7 Our proof is based on the asymptotic property of nonlinear time-series models established by Pötscher and Prucha (1997). In particular, we use the consistency (Theorem 7.1) and asymptotic normality (Theorem 11.2 (b)) of general M-estimators, defined as follows under their own notations:

$$\hat{\beta}_n \equiv \arg \min_{\beta} \vartheta_n \left(n^{-1} \sum_{t=1}^n q_t(\mathbf{z}_t, \hat{\tau}_n, \beta), \hat{\tau}_n, \beta \right), \quad (14)$$

where ϑ_n is the risk function, q_t is the contribution of data \mathbf{z}_t at time t to the risk, and $\hat{\tau}_n$ is an estimator of (potential) nuisance parameter τ . To help readers cross-reference between the book and our proof, we explain which component in our MLE setting corresponds to which in Eq. (14) as follows:

- the number of data points n is T in our setting,

- the risk function ϑ_n is given by $\vartheta_n(c, \tau, \beta) = c$ in our setting,
- the risk contribution q_t at time t is the negative log-likelihood contribution ℓ_t in our setting, that is $\ell_t(\theta) = \log p_{Y_t}(Y_t|\bar{A}_t, \theta)$, where $p_{Y_t}(\cdot|\bar{A}_t, \theta)$ is the pdf of Y_t conditional on \bar{A}_t under our model with parameter θ ,
- the data point z_t at each time t is Y_t in our setting,
- the parameter β and its estimate $\hat{\beta}_n$ correspond to θ and $\hat{\theta}$ in our setting, and
- the nuisance parameter τ and its estimate $\hat{\tau}_n$ can be disregarded in our setting.

We first prove the consistency of $\hat{\theta}$. To make the dependence of $\hat{\theta}$ on T clear, we use the notation $\hat{\theta}_T$ for $\hat{\theta}$. The consistency theorem (Theorem 7.1 of Pötscher and Prucha, 1997) was established under assumptions 7.1, 7.2 therein and the assumption about identifiably unique sequence of minimizers, which consist the common assumption set in the MLE theory. Below we show that all of their assumptions are met almost surely conditional on \bar{A}_T under our setting with given assumptions. Their assumption 7.1 (a) about the compact parameter space assumption is met almost surely by our Definition 5.5 and Assumption 5.4 as shown in Lemma B.1, 7.1 (b) about the equicontinuity of ϑ_n by $\vartheta_n(c, \tau, \beta) = c$, 7.1 (d) about the mixingness of data points by our Assumption 5.2, and 7.1 (e) by the absence of nuisance parameter in our model. The tightness in their assumption 7.2 follows the second part of our Assumption 5.3. The assumption about identifiably unique sequence of minimizers follows our Assumption 5.6. Now it suffices to show the almost sure validity of their assumption 7.1 (c) and the equicontinuity in their assumption 7.2:

- (a) $\sup_T \frac{1}{T} \sum_{t=1}^T \mathbb{E}[\sup_{\theta \in \Theta} |\log p_{Y_t}(Y_t; \theta)|^{1+\zeta} | \bar{A}_t] < \infty$ for some $\zeta > 0$; and
(b) for any fixed $y \in \mathbb{N}_0$, $\{\log p_{Y_t}(y | \bar{A}_t, \theta) : t \in (0, \infty)\}$ is equicontinuous on Θ .

This requires essential boundedness of reproduction numbers $R(\bar{A}_t, \beta)$ and scale parameter ν , which we have shown in Lemma B.1. For the Normal distribution, $\log p_{Y_t}(y | \bar{A}_t, \theta) = -\log \nu - \frac{(y - m_t(\beta, \mu))^2}{2\nu^2}$, where $m_t(\beta, \mu) \equiv \mathbb{E}_\theta[Y_t | \bar{A}_t]$. Because Θ is compact almost surely, and $(\beta, \mu, \nu) \in \Theta$ implies that $m_t(\beta, \mu)$'s are uniformly bounded away from 0 and ∞ , taking $\zeta = \frac{\gamma}{2} - 1$,

$$\sup_{\theta \in \Theta} \mathbb{E}[d_t(Y_t)^{1+\zeta}] \leq 2^{1+\zeta} \sup_{\theta \in \Theta} \left(|\log \nu|^{1+\zeta} + \frac{\mathbb{E}[Y_t^\gamma] + (m_t(\beta, \mu))^\gamma}{\nu^\gamma} \right) < \infty,$$

almost surely. For the NB distribution, $\log p_{Y_t}(y | \bar{A}_t, \theta) = \sum_{k=1}^y \log(1 + \frac{\nu-1}{k}) + \nu \log \nu + y \log m_t(\beta, \mu) - (\nu + y) \log(\nu + m_t(\beta, \mu))$ for $y \in \mathbb{N}_0$. Because $\left| \sum_{k=1}^{Y_t} \log(1 + \frac{\nu-1}{k}) \right| \leq |Y_t \log \nu|$, where $\zeta = \gamma - 1$

$$\begin{aligned} \sup_{\theta \in \Theta} \mathbb{E}[d_t(Y_t)^{1+\zeta}] &\leq 3^{1+\zeta} \sup_{\theta \in \Theta} \left[\left(\nu \log \frac{\nu + m_t(\beta, \mu)}{\nu} \right)^{1+\zeta} + \mathbb{E}[Y_t^\gamma] \left(|\log \nu|^\gamma + \left(\log \frac{\nu + m_t(\beta, \mu)}{m_t(\beta, \mu)} \right)^\gamma \right) \right] \\ &< \infty, \end{aligned}$$

almost surely. In sum, for the both cases, their assumption 7.1 (c) holds.

For the equicontinuity in their assumption 7.2, we note that $\log p_{Y_t}(y | \bar{A}_t, \theta) = f(\nu, m_t(\beta, \mu); y, \bar{A}_t)$ for a fixed function f in both cases of the Normal and NB distributions. So it is sufficient to show that $m_t(\beta, \mu)$ is equicontinuous on Θ . The equicontinuity of m_t is implied almost surely by our Definition 5.5 of Θ because

$$\sup_t \sup_{\theta \in \Theta} \|\nabla_\theta \mathbb{E}_\theta[I_t | \bar{A}_t]\|_\infty < \infty.$$

In sum, $\widehat{\theta}_T$ is consistent to θ^* conditional on \overline{A}_T almost surely: for any $\delta > 0$,

$$\lim_{T \rightarrow \infty} \mathbb{P}[\|\widehat{\theta}_T - \theta^*\| > \delta | \overline{A}_T] = 0,$$

almost surely. By Fubini's theorem,

$$\begin{aligned} \lim_{T \rightarrow \infty} \mathbb{P}[\|\widehat{\theta}_T - \theta^*\| > \delta] &= \lim_{T \rightarrow \infty} \int \mathbb{P}[\|\widehat{\theta}_T - \theta^*\| > \delta | \overline{A}_T] dP_{\overline{A}} \\ &= \int \lim_{T \rightarrow \infty} \mathbb{P}[\|\widehat{\theta}_T - \theta^*\| > \delta | \overline{A}_T] dP_{\overline{A}} \\ &= \int 0 dP_{\overline{A}} = 0. \end{aligned}$$

This concludes our proof for the consistency of $\widehat{\theta}_T$.

Now we move on to the asymptotic normality of $\widehat{\theta}_T$. The asymptotic normality (Theorem 11.2 (b) of Pötscher and Prucha, 1997) was established under assumptions 11.1, 11.2, 11.3 and 11.5 therein. We again show that all of their assumptions are met almost surely conditional on \overline{A}_T under our setting with given assumptions. Their assumption 11.1 (a) is held almost surely by our Definition 5.5 of $\Theta \in \mathbb{R}^{d+2}$ where d is the dimension of covariates A_t , 11.1 (b) by the twice differentiability of the negative log-likelihood contribution ℓ_t with respect to θ , 11.1 (c) by our definition of MLE $\widehat{\theta}_T$ as the minimizer of the risk function, 11.1 (d) by the previously shown consistency of $\widehat{\theta}_T$, 11.1(e) by the mixing condition of Y_t in our Assumption 5.2, and 11.1(f) by the second part of our Assumption 5.3. Their assumption 11.3 (a) follows the definition of θ_T^* as the minimizer of $\mathbb{E}[\sum_{t=1}^T \ell_t(\theta) | \overline{A}_T]$, and 11.3 (c, d) follows our Assumption 5.6. Their assumption 11.3 (b) is satisfied trivially by the absence of nuisance parameter in our setting. Their other assumptions 11.2 and 11.5, namely,

- (a) $\sup_T \frac{1}{T} \sum_{t=1}^T \mathbb{E}[\sup_{\theta \in \Theta} |\nabla_{\theta}^2 \ell_t(\theta)|^{1+\zeta} | \overline{A}_t] < \infty$ for some $\zeta > 0$; and
- (b) $\sup_T \sup_t \mathbb{E}[|\nabla_{\theta} \ell_t(\theta_T^*)|^{\gamma} | \overline{A}_t] < \infty$,

are weaker versions of their assumptions 13.1 and 11.5*, respectively, which are used in their consistency result of the HAC variance estimator. We relegate their almost sure validaitions to the proof of Proposition 5.8.

As a result, $\widehat{\theta}_T$ satisfies conditional asymptotic normality almost surely: for some collection \mathcal{U} of subsets in \mathbb{R}^d , with probability 1,

$$\lim_{T \rightarrow \infty} \mathbb{P}[T^{1/2} \Upsilon^{-1/2} (\widehat{\theta} - \theta^*) \in U | \overline{A}_T] = \mathbb{P}[Z_d \in U], \quad \forall U \in \mathcal{U}$$

where Z_d is an independent d -dimensional standard Normal random variable. By Fubini's theorem,

$$\begin{aligned} \lim_{T \rightarrow \infty} \mathbb{P}[T^{1/2} \Upsilon^{-1/2} (\widehat{\theta} - \theta^*) \in U] &= \lim_{T \rightarrow \infty} \int \mathbb{P}[T^{1/2} \Upsilon^{-1/2} (\widehat{\theta} - \theta^*) \in U | \overline{A}_T] dP_{\overline{A}} \\ &= \int \lim_{T \rightarrow \infty} \mathbb{P}[T^{1/2} \Upsilon^{-1/2} (\widehat{\theta} - \theta^*) \in U | \overline{A}_T] dP_{\overline{A}} \\ &= \int \mathbb{P}[Z_d \in U] dP_{\overline{A}} = \mathbb{P}[Z_d \in U]. \end{aligned}$$

This concludes the proof of asymptotic normality.

Proof of Proposition 5.8 We use the consistency result of the HAC variance estimator established by Pötscher and Prucha (1997). The corresponding theorem (Theorem 13.1 (b)

therein) uses assumptions 11.1, 11.2, 11.3*, 11.5* and 13.1 therein. We already checked their assumptions 11.1, 11.2 and 11.3 in the proof of Theorem 5.7. Their assumption 11.3* is stronger than 11.3 by necessitating $\mathbb{E}[\nabla_{\theta}\ell_t(\theta_T^*)] = 0$ at each t , rather than $\sum_t \mathbb{E}[\nabla_{\theta}\ell_{t=1}^T(\theta_T^*)] = 0$. This essentially means that the true mean $\mathbb{E}[Y_t|A_t]$ is correctly specified by the model mean $\mathbb{E}_{\theta}[Y_t|A_t]$ at $\theta = \theta^*$. That is why our Proposition 5.9 requires the additional assumption. Now it suffices to validate their assumptions 11.5* and 13.1, namely,

- (i) $\nabla_{\theta}\ell_t(\theta^*)$ is near epoch dependent of size $-2(r-1)/(r-2)$ on an α -mixing baseline process with coefficient of size $-2r/(r-2)$;
- (ii) $\sup_T \sup_t \mathbb{E}[|\nabla_{\theta}\ell_t(\theta_T^*)|^{2\gamma}|\bar{A}_t] < \infty$;
- (iii) $\sup_T \frac{1}{T} \sum_{t=1}^T \mathbb{E}[\sup_{\theta \in \Theta} |\nabla_{\theta}\ell_t(\theta)|^2|\bar{A}_t] < \infty$; and
- (iv) $\sup_T \frac{1}{T} \sum_{t=1}^T \mathbb{E}[\sup_{\theta \in \Theta} |\nabla_{\theta}^2\ell_t(\theta)|^2|\bar{A}_t] < \infty$,

in almost sure sense.

Part (i) follows our Assumption 5.2 about the mixingness of the data points. For parts (ii) – (iv), it is sufficient to show that $\nabla_{(\nu, m_t)}\ell_t(\theta_T^*)$ has a finite 2γ -moment and that $\sup_{\theta \in \Theta} \nabla_{(\nu, m_t)}\ell_t(\theta)$ and $\sup_{\theta \in \Theta} \nabla_{(\nu, m_t)}^2\ell_t(\theta)$ have finite 2-moments, because

$$\begin{aligned} \sup_t \sup_{\theta \in \Theta} \|\nabla_{\theta}\mathbb{E}_{\theta}[I_t|\bar{A}_t]\|_{\infty} &< \infty, \\ \sup_t \sup_{\theta \in \Theta} \|\nabla_{\theta}^2\mathbb{E}_{\theta}[I_t|\bar{A}_t]\|_{\infty} &< \infty \end{aligned}$$

and Definition 5.5 implies

$$\sup_t \sup_{\theta \in \Theta} \|\nabla_{\theta}m_t\|_{\infty} < \infty \text{ and } \sup_t \sup_{\theta \in \Theta} \|\nabla_{\theta}^2m_t\|_{\infty} < \infty.$$

For the Normal distribution, the derivatives are

$$\begin{aligned} \frac{\partial \ell_t(\theta)}{\partial \nu} &= -\frac{1}{\nu} + \frac{1}{\nu^3}(Y_t - m_t)^2, \\ \frac{\partial \ell_t(\theta)}{\partial m_t} &= \frac{1}{\nu^2}(Y_t - m_t), \\ \frac{\partial^2 \ell_t(\theta)}{\partial \nu^2} &= \frac{1}{\nu^2} - \frac{3}{\nu^4}(Y_t - m_t)^2, \\ \frac{\partial^2 \ell_t(\theta)}{\partial \nu \partial m_t} &= -\frac{2}{\nu^3}(Y_t - m_t), \\ \frac{\partial^2 \ell_t(\theta)}{\partial m_t^2} &= -\frac{1}{\nu^2}. \end{aligned}$$

By our Assumption 5.3 and Definition 5.5, $\nabla_{(\nu, m_t)}\ell_t(\theta_T^*)$ has a finite 2γ -moment, and $\sup_{\theta \in \Theta} \nabla_{(\nu, m_t)}\ell_t(\theta)$ and $\sup_{\theta \in \Theta} \nabla_{(\nu, m_t)}^2\ell_t(\theta)$ have finite 2-moments almost surely.

For the NB distribution, the derivatives are

$$\begin{aligned}\frac{\partial \ell_t(\theta)}{\partial \nu} &= \sum_{k=1}^{Y_t} \frac{1}{k + \nu - 1} + \log \nu + 1 - \log(\nu + m_t) - \frac{\nu + Y_t}{\nu + m_t}, \\ \frac{\partial \ell_t(\theta)}{\partial m_t} &= \frac{Y_t}{m_t} - \frac{\nu + Y_t}{\nu + m_t}, \\ \frac{\partial^2 \ell_t(\theta)}{\partial \nu^2} &= -\sum_{k=1}^{Y_t} \frac{1}{(k + \nu - 1)^2} + \frac{1}{\nu} - \frac{1}{\nu + m_t} + \frac{Y_t - m_t}{(\nu + m_t)^2}, \\ \frac{\partial^2 \ell_t(\theta)}{\partial \nu \partial m_t} &= \frac{Y_t - m_t}{(\nu + m_t)^2}, \\ \frac{\partial^2 \ell_t(\theta)}{\partial m_t^2} &= \frac{r + Y_t}{(r + m_t)^2} - \frac{Y_t}{m_t^2}.\end{aligned}$$

Based on our observation that

$$\begin{aligned}\sum_{k=1}^{Y_t} \frac{1}{k + \nu - 1} &\leq \frac{Y_t}{\nu}, \\ \sum_{k=1}^{Y_t} \frac{1}{(k + \nu - 1)^2} &\leq \frac{Y_t}{\nu^2},\end{aligned}$$

Assumption 5.3 and Definition 5.5 implies $\nabla_{(\nu, m_t)} \ell_t(\theta_T^*)$ has a finite 2γ -moment and $\sup_{\theta \in \Theta} \nabla_{(\nu, m_t)} \ell_t(\theta)$ and $\sup_{\theta \in \Theta} \nabla_{(\nu, m_t)}^2 \ell_t(\theta)$ have finite 2-moments almost surely.

In sum, the HAC variance estimator $\hat{\Upsilon}$ is almost surely consistent to Υ conditional on \bar{A}_T : for any $\delta > 0$,

$$\lim_{T \rightarrow \infty} \mathbb{P}[\|\hat{\Upsilon} - \Upsilon\| > \delta | \bar{A}_T] = 0,$$

almost surely. By Fubini's theorem,

$$\begin{aligned}\lim_{T \rightarrow \infty} \mathbb{P}[\|\hat{\Upsilon} - \Upsilon\| > \delta] &= \lim_{T \rightarrow \infty} \int \mathbb{P}[\|\hat{\Upsilon} - \Upsilon\| > \delta | \bar{A}_T] dP_{\bar{A}} \\ &= \int \lim_{T \rightarrow \infty} \mathbb{P}[\|\hat{\Upsilon} - \Upsilon\| > \delta | \bar{A}_T] dP_{\bar{A}} \\ &= \int 0 dP_{\bar{A}} = 0.\end{aligned}$$

This concludes our proof for the consistency of $\hat{\Upsilon}$.

B.2. Lemmas and Proofs for Section 6

In this appendix, we provide supplementary lemmas for the theoretical arguments regarding the asymptotic convergence of the robust empirical Bayesian confidence regions proposed in Section 6.

LEMMA B.2. *The collection $\{r_0(u, \chi), r_1(u, \chi), \dots\}$ of functions is uniformly equicontinuous with respect to both u and χ .*

PROOF. Due to the uniform continuity of the Normal distribution, it is easy to show that r_0 is uniformly continuous. So for any $\epsilon > 0$, we can find $\delta > 0$ such that $|u - u'| < \delta$ and $|\chi^2 - \chi'^2| < \delta$ imply $|r_0(u, \chi) - r_0(u', \chi')| < \epsilon$.

For any $d > 0$, based on Eq. (7), $r_{d-1}(u, \chi) = \mathbb{E}_{\chi_{d-1}}[r_0(u, \sqrt{\chi^2 - \chi_{d-1}^2})]$, where χ_{d-1}^2 is a χ^2 random variable with degree of freedom $d - 1$. Hence, for the δ defined above, $|u - u'| < \delta$ and

$|\chi^2 - \chi'^2| < \delta$ imply

$$\begin{aligned} |r_{d-1}(u, \chi) - r_{d-1}(u', \chi')| &= |\mathbb{E}[r_0(u, \sqrt{\chi^2 - \chi_{d-1}^2}) | \chi_{d-1}] - \mathbb{E}[r_0(u', \sqrt{\chi'^2 - \chi_{d-1}^2})]| \\ &\leq \mathbb{E}_{\chi_{d-1}}[|r_0(u, \sqrt{\chi^2 - \chi_{d-1}^2}) - r_0(u', \sqrt{\chi'^2 - \chi_{d-1}^2})|] \\ &\leq \mathbb{E}_{\chi_{d-1}}[\epsilon] = \epsilon \end{aligned}$$

because $(\sqrt{\chi^2 - \chi_{d-1}^2})^2 - (\sqrt{\chi'^2 - \chi_{d-1}^2})^2 < \delta$ almost surely. \square

Suppose that

$$\mathcal{M} \equiv \left\{ (m^{(2)}, m^{(4)}) : m^{(2)} = \int u dF(u), m^{(4)} = \int u^2 dF(u), F \in \mathcal{F} \right\}.$$

In light of Hölder's inequality, it is easy to see that

$$\mathcal{M} = \{(m^{(2)}, m^{(4)}) \in (0, \infty) \times (0, \infty) : m^{(4)} \geq m^{(2)2}\} \cup \{(0, 0)\}.$$

LEMMA B.3. $\rho_{m^{(2)}, m^{(4)}}(\chi)$ is continuous in $[0, \infty)$. Furthermore, $\rho_{m^{(2)}, m^{(4)}}(\chi)$ is continuous with respect to $(m^{(2)}, m^{(4)})$ in \mathcal{M} .

PROOF. For the continuity with respect to χ ,

$$|\rho_{m^{(2)}, m^{(4)}}(\chi_1) - \rho_{m^{(2)}, m^{(4)}}(\chi_2)| \leq \sup_{F \in \mathcal{F}_{m^{(2)}, m^{(4)}}} \int |r_{d-1}(u, \chi_1) - r_{d-1}(u, \chi_2)| dF(u),$$

where $\mathcal{F}_{m^{(2)}, m^{(4)}} \equiv \{F \in \mathcal{F} : \int u dF(u) = m^{(2)}, \int u^2 dF(u) = m^{(4)}\}$. Due to the uniform continuity of r_{d-1} ,

$$\sup_{u \in [0, \infty)} |r_{d-1}(u, \chi_1) - r_{d-1}(u, \chi_2)| \leq C|\chi_1 - \chi_2|$$

for some constant $C > 0$. This shows the continuity with respect to χ in $[0, \infty)$.

For the continuity with respect to $(m^{(2)}, m^{(4)})$, we first consider the case where $m^{(4)} > m^{(2)2} > 0$. Then, $(m^{(2)}, m^{(4)})$ is in the interior of \mathcal{M} . So by the duality theorem in Smith (1995), for $(m^{(2)'}, m^{(4)'})$ in a small enough neighborhood of $(m^{(2)}, m^{(4)})$,

$$\begin{aligned} \rho_{m^{(2)'}, m^{(4)'}}(\chi) &= \inf_{\lambda_0, \lambda_1, \lambda_2} \lambda_0 + \lambda_1 m^{(2)'} + \lambda_2 m^{(4)'} \\ \text{s.t. } \lambda_0 + \lambda_1 u + \lambda_2 u^2 &\geq r_{d-1}(u, \chi) \quad \text{for all } u \in [0, \infty), \end{aligned}$$

and the infimum is finite. As the infimum of the collection of affine functions, $\rho_{m^{(2)}, m^{(4)}}(\chi)$ is a convex function of $(m^{(2)}, m^{(4)})$ in the neighborhood and hence is continuous.

Now, consider the case where $m^{(4)} = m^{(2)2} \geq 0$. Then for $F \in \mathcal{F}_{m^{(2)}, m^{(4)}}$, $u \sim F$ is almost surely $m^{(2)}$. As a result, $\rho_{m^{(2)}, m^{(4)}}(\chi) = r_{d-1}(m^{(2)}, \chi)$ and is continuous in $\partial\mathcal{M} \equiv \{(m^{(2)}, m^{(4)}) \in \mathcal{M} : m^{(4)} = m^{(2)2} \geq 0\}$. It is now sufficient to show that $\rho_{m^{(2)}, m^{(4)}}(\chi)$ is continuous with respect to $m^{(4)}$ at $m^{(4)} = m^{(2)2}$. For any $\epsilon > 0$, suppose that $u \sim F \in \mathcal{F}_{m^{(2)}, m^{(2)2} + \epsilon^2}$. Then,

$$\mathbb{E}[(u - m^{(2)})^2] = \mathbb{E}[u^2] - 2\mathbb{E}[u]m^{(2)} + m^{(2)2} = (m^{(2)2} + \epsilon^2) - 2m^{(2)2} + m^{(2)2} = \epsilon^2.$$

By Markov's inequality, $\mathbb{P}[|u - m^{(2)}| > \sqrt{\epsilon}] \leq \epsilon$, and

$$\begin{aligned}
& \mathbb{P}[\chi_{d-1}^2 + (Z - \sqrt{u})^2 \geq \chi^2] \\
& \leq \mathbb{P}[\chi_{d-1}^2 + (Z - \sqrt{u})^2 \geq \chi^2, |u - m^{(2)}| \leq \sqrt{\epsilon}] + \mathbb{P}[|u - m^{(2)}| > \sqrt{\epsilon}] \\
& \leq \mathbb{P}[\chi_{d-1}^2 + (Z - \sqrt{u})^2 \geq \chi^2, |(Z - \sqrt{u})^2 - (Z - m^{(2)})^2| \leq \epsilon^{1/4} + \epsilon^{1/2}] + \epsilon \\
& \leq \mathbb{P}[\chi_{d-1}^2 + (Z - m^{(2)})^2 \geq \chi^2 - \epsilon^{1/4} - \epsilon^{1/2}] + \epsilon \\
& = \rho_{m^{(2)}, m^{(2)2}} \left(\sqrt{\chi^2 - \epsilon^{1/4} - \epsilon^{1/2}} \right) + \epsilon,
\end{aligned}$$

where χ_{d-1}^2 and Z are a χ^2 random variable with degree of freedom $d - 1$ and a univariate standard Gaussian random variable. Taking the supremum over $F \in \mathcal{F}_{m^{(2)}, m^{(4)}}$, we get $\rho_{m^{(2)}, m^{(2)2} + \epsilon^2}(\chi) \leq \rho_{m^{(2)}, m^{(2)2}}(\sqrt{\chi^2 - \epsilon^{1/4} - \epsilon^{1/2}}) + \epsilon$. Similarly, we get $\rho_{m^{(2)}, m^{(2)2} + \epsilon^2}(\chi) \geq \rho_{m^{(2)}, m^{(2)2}}(\sqrt{\chi^2 + \epsilon^{1/4} + \epsilon^{1/2}}) - \epsilon$. Because $\rho_{m^{(2)}, m^{(2)2}}(\chi)$ is continuous with respect to χ , we get $\lim_{\epsilon \rightarrow 0^+} \rho_{m^{(2)}, m^{(2)2} + \epsilon}(\chi) = \rho_{m^{(2)}, m^{(2)2}}(\chi)$. This proves the desired claim. \square

LEMMA B.4. *Let \mathcal{M}^o be a compact subset of \mathcal{M} . Then $\lim_{\chi \rightarrow \infty} \sup_{\mathcal{M}^o} \rho_{m^{(2)}, m^{(4)}}(\chi) = 0$, and $\rho_{m^{(2)}, m^{(4)}}(\chi)$ is uniformly continuous with respect to $(\chi, m^{(2)}, m^{(4)})$ in $[0, \infty) \times \mathcal{M}^o$.*

PROOF. The first claim follows by Markov's inequality and compactness of \mathcal{M}^o . Specifically, because $\mathbb{E}_{u \sim F}[\chi_{d-1}^2 + (Z - \sqrt{u})^2] = d + \mathbb{E}_{u \sim F}[u]$, by Markov's inequality

$$\begin{aligned}
\rho_{m^{(2)}, m^{(4)}}(\chi) &= \sup_{F \in \mathcal{F}_{m^{(2)}, m^{(4)}}} \mathbb{P}_{u \sim F}[\chi_{d-1}^2 + (Z - \sqrt{u})^2 \geq \chi^2] \\
&\leq \sup_{F \in \mathcal{F}_{m^{(2)}, m^{(4)}}} \frac{1}{\chi^2} \mathbb{E}_{u \sim F}[\chi_{d-1}^2 + (Z - \sqrt{u})^2] \\
&= \sup_{F \in \mathcal{F}_{m^{(2)}, m^{(4)}}} \frac{1}{\chi^2} (d + \mathbb{E}_{u \sim F}[u]) = \frac{d + m^{(2)}}{\chi^2}.
\end{aligned}$$

So the compactness of \mathcal{M}^o implies that $\sup_{\mathcal{M}^o} m^{(2)} < \infty$, and $\lim_{\chi \rightarrow \infty} \sup_{\mathcal{M}^o} \rho_{m^{(2)}, m^{(4)}}(\chi) = 0$.

Now given $\epsilon > 0$, let $\bar{\chi}$ be large enough so that $\chi \geq \bar{\chi} \implies \rho_{m^{(2)}, m^{(4)}}(\chi) < \epsilon$. By Lemma B.3, $\rho_{m^{(2)}, m^{(4)}}(\chi)$ is continuous on $[0, \bar{\chi} + 1] \times \mathcal{M}^o$. Suppose that $(\chi_k, m_k^{(2)}, m_k^{(4)}) \in [0, \infty) \times \mathcal{M}^o$ for $k = 1, 2$. If both χ_1 and χ_2 are in $[0, \bar{\chi} + 1]$, due to the compactness of $[0, \bar{\chi} + 1] \times \mathcal{M}^o$, there exists $\delta < 1$ such that

$$\max\{|\chi_1 - \chi_2|, |m_1^{(2)}, m_2^{(2)}|, |m_1^{(4)}, m_2^{(4)}|\} \leq \delta \implies |\rho_{m_1^{(2)}, m_1^{(4)}}(\chi_1) - \rho_{m_2^{(2)}, m_2^{(4)}}(\chi_2)| \leq \epsilon.$$

On the other hand, if (without loss of generality) $\chi_1 > \bar{\chi} + 1$,

$$\begin{aligned}
& \max\{|\chi_1 - \chi_2|, |m_1^{(2)}, m_2^{(2)}|, |m_1^{(4)}, m_2^{(4)}|\} \leq \delta \implies \chi_2 > \bar{\chi} \\
& \implies |\rho_{m_1^{(2)}, m_1^{(4)}}(\chi_1) - \rho_{m_2^{(2)}, m_2^{(4)}}(\chi_2)| \leq |\rho_{m_1^{(2)}, m_1^{(4)}}(\chi_1)| + |\rho_{m_2^{(2)}, m_2^{(4)}}(\chi_2)| \leq 2\epsilon.
\end{aligned}$$

In sum, $\rho_{m^{(2)}, m^{(4)}}(\chi)$ is uniformly continuous with respect to $(\chi, m^{(2)}, m^{(4)})$ in $[0, \infty) \times \mathcal{M}^o$. \square

Proof of Theorem 6.5 First, we show that for any deterministic $\chi_{[1], \dots, \chi_{[N]}$, subset \mathcal{X} of \mathcal{A} and $\epsilon > 0$, there exists $\bar{N}_{\mathcal{X}}$ such that $N_{\mathcal{X}} \geq \bar{N}_{\mathcal{X}}$ implies

$$\frac{1}{N_{\mathcal{X}}} \left(\sum_{j \in \mathcal{I}_{\mathcal{X}}} \mathbb{P}[\|T_{[j]}^{1/2} (\widehat{W}_{[j]} \widehat{\Upsilon}_{[j]}^{1/2})^{-1} (\tilde{\theta}_{[j]} - \theta_{[j]})\|_2 > \chi_{[j]} |\theta_{[1], \dots, [N]}, \Upsilon_{[1], \dots, [N]}|] \right) < \epsilon, \quad (15)$$

where $\widehat{W}_{[j]} \equiv \widehat{\Phi}^{(2)}(\widehat{\Phi}^{(2)} + T_{[j]}^{-1}\widehat{\Upsilon}_{[j]})^{-1}$, $\mathcal{I}_{\mathcal{X}} \equiv \{j : \Upsilon_{[j]} \in \mathcal{X}\}$ and $N_{\mathcal{X}} \equiv |\mathcal{I}_{\mathcal{X}}|$. For the first term,

$$\begin{aligned} T_{[j]}^{1/2}(\widehat{W}_{[j]}\widehat{\Upsilon}_{[j]}^{1/2})^{-1}(\tilde{\theta}_{[j]} - \theta_{[j]}) &= T_{[j]}^{1/2}(\widehat{W}_{[j]}\widehat{\Upsilon}_{[j]}^{1/2})^{-1}(\widehat{\theta}_o + \widehat{W}_{[j]}(\widehat{\theta}_{[j]} - \widehat{\theta}_o) - \theta_{[j]}) \\ &= T_{[j]}^{1/2}\widehat{\Upsilon}_{[j]}^{-1/2}(\widehat{\theta}_{[j]} - \theta_{[j]}) + T_{[j]}^{1/2}(\widehat{W}_{[j]}\widehat{\Upsilon}_{[j]}^{1/2})^{-1}(id - \widehat{W}_{[j]})(\widehat{\theta}_o - \theta_{[j]}) \\ &= T_{[j]}^{1/2}\widehat{\Upsilon}_{[j]}^{-1/2}(\widehat{\theta}_{[j]} - \theta_{[j]}) + \widehat{b}_{[j]}, \end{aligned}$$

where $\widehat{b}_{[j]} \equiv -T_{[j]}^{-1/2}\widehat{\Upsilon}_{[j]}^{1/2}\widehat{\Phi}^{(2)-1}(\theta_{[j]} - \widehat{\theta}_o)$. For any $\delta > 0$, $\frac{1}{N_{\mathcal{X}}} \sum_{j \in \mathcal{I}_{\mathcal{X}}} \mathbb{I}\{\|T_{[j]}^{1/2}(\widehat{W}_{[j]}\widehat{\Upsilon}_{[j]}^{1/2})^{-1}(\tilde{\theta}_{[j]} - \theta_{[j]}) - \widehat{b}_{[j]}\|_2 > \chi_{[j]}\}$ is upper bounded by

$$\begin{aligned} &\frac{1}{N_{\mathcal{X}}} \sum_{j \in \mathcal{I}_{\mathcal{X}}} \mathbb{I}\{\|T_{[j]}^{1/2}(\widehat{W}_{[j]}\widehat{\Upsilon}_{[j]}^{1/2})^{-1}(\tilde{\theta}_{[j]} - \theta_{[j]}) - \widehat{b}_{[j]} + b_{[j]}\|_2 > \chi_{[j]} - \delta\} \\ &+ \frac{1}{N_{\mathcal{X}}} \sum_{j \in \mathcal{I}_{\mathcal{X}}} \mathbb{I}\{\|\widehat{b}_{[j]} - b_{[j]}\|_2 \geq \delta\}. \end{aligned}$$

Because Assumption 6.1 implies that $(T_{[j]}^{1/2}\widehat{W}_{[j]}\widehat{\Upsilon}_{[j]}^{1/2})^{-1}(\tilde{\theta}_{[j]} - \theta_{[j]}) - \widehat{b}_{[j]} = T_{[j]}^{1/2}\widehat{\Upsilon}_{[j]}^{-1/2}(\widehat{\theta}_{[j]} - \theta_{[j]}) \stackrel{d}{\rightarrow} Z_d$ conditional on $\theta_{[1, \dots, N]}$ and $\Upsilon_{[1, \dots, N]}$, where Z_d is the d -dimensional standard Normal random variable, there exists $\overline{N}_{\mathcal{X}}^{(1)}$ such that $N_{\mathcal{X}} \geq \overline{N}_{\mathcal{X}}^{(1)}$ implies

$$\begin{aligned} &\frac{1}{N_{\mathcal{X}}} \sum_{j \in \mathcal{I}_{\mathcal{X}}} \mathbb{P}[\|T_{[j]}^{1/2}(\widehat{W}_{[j]}\widehat{\Upsilon}_{[j]}^{1/2})^{-1}(\tilde{\theta}_{[j]} - \theta_{[j]}) - \widehat{b}_{[j]} + b_{[j]}\|_2 > \chi_{[j]} - \delta | \theta_{[1, \dots, N]}, \Upsilon_{[1, \dots, N]}] \\ &- \frac{1}{N_{\mathcal{X}}} \sum_{j \in \mathcal{I}_{\mathcal{X}}} r_{d-1}(b_{[j]}, \chi_{[j]} - \delta) \leq \epsilon. \end{aligned}$$

On the other hand, by Assumption 6.3 and Markov's inequality, we can take $C > 0$ such that

$$\frac{1}{N_{\mathcal{X}}} \sum_{j \in \mathcal{I}_{\mathcal{X}}} \mathbb{I}\{\|\theta_{[j]}\|_2 > C\} \leq \epsilon.$$

Then,

$$\begin{aligned} &\frac{1}{N_{\mathcal{X}}} \sum_{j \in \mathcal{I}_{\mathcal{X}}} \mathbb{P}[\|\widehat{b}_{[j]} - b_{[j]}\|_2 \geq \delta | \theta_{[1, \dots, N]}, \Upsilon_{[1, \dots, N]}] \\ &\leq \frac{1}{N_{\mathcal{X}}} \sum_{j \in \mathcal{I}_{\mathcal{X}}} \mathbb{P}[\|\widehat{b}_{[j]} - b_{[j]}\|_2 \geq \delta | \theta_{[1, \dots, N]}, \Upsilon_{[1, \dots, N]}] \mathbb{I}\{\|\theta_{[j]}\|_2 \leq C\} + \frac{1}{N_{\mathcal{X}}} \sum_{j \in \mathcal{I}_{\mathcal{X}}} \mathbb{I}\{\|\theta_{[j]}\|_2 > C\} \\ &\leq \frac{1}{N_{\mathcal{X}}} \sum_{j \in \mathcal{I}_{\mathcal{X}}} \mathbb{P}[\|\widehat{b}_{[j]} - b_{[j]}\|_2 \geq \delta | \theta_{[1, \dots, N]}, \Upsilon_{[1, \dots, N]}] \mathbb{I}\{\|\theta_{[j]}\|_2 \leq C\} + \epsilon. \end{aligned}$$

The eigenvalue conditions in Assumption 6.3 imply that $\|\widehat{b}_{[j]} - b_{[j]}\|_2 \leq T_{[j]}^{-1/2}\{C\lambda_{\max,*}(\|\widehat{\Upsilon}_{[j]}^{1/2} - \Upsilon_{[j]}^{1/2}\|_{\text{op}} + \|\widehat{\Phi}^{(2)-1} - \Phi^{(2)-1}\|_{\text{op}}) + \lambda_{\max,*}^2\|\widehat{\theta}_o - \theta_o\|_2\}$ for j satisfying $\|\theta_{[j]}\|_2 \leq C$, and Assumption 6.4 implies that for some $\overline{N}_{\mathcal{X}}^{(2)}$,

$$N_{\mathcal{X}} \geq \overline{N}_{\mathcal{X}}^{(2)} \implies \frac{1}{N_{\mathcal{X}}} \sum_{j \in \mathcal{I}_{\mathcal{X}}} \mathbb{P}[\|\widehat{b}_{[j]} - b_{[j]}\|_2 \geq \delta | \theta_{[1, \dots, N]}, \Upsilon_{[1, \dots, N]}] \leq \epsilon.$$

In summary, for $N_{\mathcal{X}} \geq \max\{\bar{N}_{\mathcal{X}}^{(1)}, \bar{N}_{\mathcal{X}}^{(2)}\}$,

$$\begin{aligned} & \frac{1}{N_{\mathcal{X}}} \sum_{j \in \mathcal{I}_{\mathcal{X}}} \mathbb{P}[\|T_{[j]}^{1/2}(\widehat{W}_{[j]}\widehat{\Upsilon}_{[j]}^{1/2})^{-1}(\tilde{\theta}_{[j]} - \theta_{[j]})\|_2 > \chi_{[j]}|\theta_{[1,\dots,N]}, \Upsilon_{[1,\dots,N]}] \\ & \leq \frac{1}{N_{\mathcal{X}}} \sum_{j \in \mathcal{I}_{\mathcal{X}}} r_{d-1}(\|b_{[j]}\|_2^2, \chi_{[j]} - \delta) + 3\epsilon. \end{aligned}$$

Similarly, there exists $\bar{N}_{\mathcal{X}}$ such that $N_{\mathcal{X}} \geq \bar{N}_{\mathcal{X}}$ implies

$$\begin{aligned} & \frac{1}{N_{\mathcal{X}}} \sum_{j \in \mathcal{I}_{\mathcal{X}}} \mathbb{P}[\|T_{[j]}^{1/2}(\widehat{W}_{[j]}\widehat{\Upsilon}_{[j]}^{1/2})^{-1}(\tilde{\theta}_{[j]} - \theta_{[j]})\|_2 > \chi_{[j]}|\theta_{[1,\dots,N]}, \Upsilon_{[1,\dots,N]}] \\ & \geq \frac{1}{N_{\mathcal{X}}} \sum_{j \in \mathcal{I}_{\mathcal{X}}} r_{d-1}(\|b_{[j]}\|_2^2, \chi_{[j]} + \delta) - 3\epsilon. \end{aligned}$$

Noting that r_0, r_1, \dots are uniformly equicontinuous, we proved the desired claim.

We proceed to the proof of the main theorem. Due to the way \mathcal{U} is defined as in Assumption 6.3, \mathcal{U} is compact. Consider the functions $m^{(2)}(\Upsilon)$ and $m^{(4)}(\Upsilon)$ defined as in Eq. (9) with Υ in place of $\Upsilon_{[j]}$. Due to the continuity of those functions and the compactness of \mathcal{U} , $\mathcal{M}^{\mathcal{U}} \equiv \{(m^{(2)}(\Upsilon), m^{(4)}(\Upsilon)) : \Upsilon \in \mathcal{U}\}$ is also compact. In the following proof, we use the uniform continuity of $\rho_{m^{(2)}, m^{(4)}}(\chi)$ with respect to $(\chi, m^{(2)}, m^{(4)})$ in $[0, \infty) \times \mathcal{M}^{\mathcal{U}}$, as stated in Lemma B.4. For the full proof of the statement, see Section 6. For $\delta > 0$, let

$$\begin{aligned} \bar{\rho}_{m^{(2)}, m^{(4)}}^{\delta}(\chi) & \equiv \sup\{\rho_{\tilde{m}^{(2)}, \tilde{m}^{(4)}}(\chi) : |\tilde{m}^{(2)} - m^{(2)}| < \delta, |\tilde{m}^{(4)} - m^{(4)}| < \delta\}, \\ \underline{\rho}_{m^{(2)}, m^{(4)}}^{\delta}(\chi) & \equiv \inf\{\rho_{\tilde{m}^{(2)}, \tilde{m}^{(4)}}(\chi) : |\tilde{m}^{(2)} - m^{(2)}| < \delta, |\tilde{m}^{(4)} - m^{(4)}| < \delta\}. \end{aligned}$$

If δ is smaller than a constant depending on $\mathcal{M}^{\mathcal{U}}$, then $\bar{\rho}_{m^{(2)}, m^{(4)}}^{\delta}(\chi)$ and $\underline{\rho}_{m^{(2)}, m^{(4)}}^{\delta}(\chi)$ are continuous in χ , and

$$\lim_{\epsilon \rightarrow 0} \sup\{\bar{\rho}_{m^{(2)}, m^{(4)}}^{\delta}(\chi) - \underline{\rho}_{m^{(2)}, m^{(4)}}^{\delta}(\chi) : \chi \in [0, \infty), (m^{(2)}, m^{(4)}) \in \mathcal{M}^{\mathcal{U}}\} = 0. \quad (16)$$

Moreover, there exists a finite number of $\|\cdot\|_{\text{op}}$ -balls $\mathcal{X}_1, \dots, \mathcal{X}_K$ covering \mathcal{U} such that $\Upsilon_{[j]} \in \mathcal{X}_k \implies |m_{[j]}^{(2)} - m^{(2)}(\mathcal{X}_k)| < \delta$ and $|m_{[j]}^{(4)} - m^{(4)}(\mathcal{X}_k)| < \delta$, where $m^{(2)}(\mathcal{X}_k)$ and $m^{(4)}(\mathcal{X}_k)$ are evaluated at the center of \mathcal{X}_k . Consider an arbitrary partition $\mathcal{I}_1, \dots, \mathcal{I}_K$ of $\mathcal{I}_{\mathcal{X}}$ such that $\mathcal{I}_k \subseteq \mathcal{I}_{\mathcal{X}} \cap \mathcal{X}_k$ for all k . By the upper claim of Eq. (15), for any $\epsilon > 0$, there exists \bar{N}_k such that $N_k \geq \bar{N}_k$ implies

$$\frac{1}{N_k} \left| \sum_{j \in \mathcal{I}_k} \mathbb{P}[\|T_{[j]}^{1/2}(\widehat{W}_{[j]}\widehat{\Upsilon}_{[j]}^{1/2})^{-1}(\tilde{\theta}_{[j]} - \theta_{[j]})\|_2 > \underline{\chi}_k|\theta_{[1,\dots,N]}, \Upsilon_{[1,\dots,N]}] - \sum_{j \in \mathcal{I}_k} r_{d-1}(\|b_{[j]}\|_2^2, \underline{\chi}_k) \right| < \epsilon, \quad (17)$$

where $N_k \equiv |\mathcal{I}_k|$ and $\underline{\chi}_k = \min\{\chi : \underline{\rho}_{m^{(2)}(\mathcal{X}_k), m^{(4)}(\mathcal{X}_k)}^{2\epsilon}(\chi) \leq \alpha\}$. Let $\bar{N}_* \equiv \max\{\bar{N}_k, k = 1, \dots, K\}$, $\mathcal{K} \equiv \{k : N_k \geq \bar{N}_*\}$ and $N_{\mathcal{K}} \equiv \sum_{k \in \mathcal{K}} N_k$. Then,

$$\frac{1}{N_{\mathcal{X}}} \sum_{j \in \mathcal{I}_{\mathcal{X}}} \mathbb{I}\{\theta_{[j]} \notin \tilde{\mathcal{C}}_{[j]}\} \leq \max_{k \in \mathcal{K}} \frac{1}{N_k} \sum_{j \in \mathcal{I}_k} \mathbb{I}\{\theta_{[j]} \notin \tilde{\mathcal{C}}_{[j]}\} + \frac{N_{\mathcal{X}} - N_{\mathcal{K}}}{N_{\mathcal{X}}}.$$

Because $N_{\mathcal{X}} - N_{\mathcal{K}}$ is upper bounded by $\bar{N}K$, $\frac{N_{\mathcal{X}} - N_{\mathcal{K}}}{N_{\mathcal{X}}} \rightarrow 0$ as $N_{\mathcal{X}} \rightarrow \infty$. On the other hand,

$$\max_{k \in \mathcal{K}} \frac{1}{N_k} \sum_{j \in \mathcal{I}_k} \mathbb{I}\{\theta_{[j]} \notin \tilde{\mathcal{C}}_{[j]}\} \leq \max_{k \in \mathcal{K}} \left[\frac{1}{N_k} \sum_{j \in \mathcal{I}_k} \mathbb{I}\{|\widehat{m}_{[j]}^{(l)} - m^{(l)}(\mathcal{X}_k)| > \epsilon \text{ for } l = 2 \text{ or } 4\} + \frac{1}{N_k} \sum_{j \in \mathcal{I}_k} \mathbb{I}\{\|T_{[j]}^{1/2}(\widehat{W}_{[j]}\widehat{\Upsilon}_{[j]}^{1/2})^{-1}(\tilde{\theta}_{[j]} - \theta_{[j]})\|_2 > \underline{\chi}_k\} \right],$$

where $\underline{\chi}_k = \min\{\chi : \underline{\rho}_{m^{(2)}(\mathcal{X}_k), m^{(4)}(\mathcal{X}_k)}^{2\epsilon}(\chi) \leq \alpha\}$. Due to the consistency of $\widehat{\Upsilon}_{[j]}$, $\widehat{\Phi}^{(2)}$ and $\widehat{\Phi}^{(4)}$ in Assumptions 6.2 and 6.4 and the homoskedasticity in Assumption 6.3, the first term converges to 0 as $N_{\mathcal{X}} \rightarrow \infty$. For the second term, Eq. (17) implies that

$$\max_{k \in \mathcal{K}} \frac{1}{N_k} \sum_{j \in \mathcal{I}_k} \mathbb{I}\{\|T_{[j]}^{1/2}(\widehat{W}_{[j]} \widehat{\Upsilon}_{[j]}^{1/2})^{-1}(\widetilde{\theta}_{[j]} - \theta_{[j]})\|_2 > \underline{\chi}_k\} \leq \max_{k \in \mathcal{K}} \frac{1}{N_k} r_{d-1}(\|b_{[j]}\|_2^2, \underline{\chi}_k) + \epsilon$$

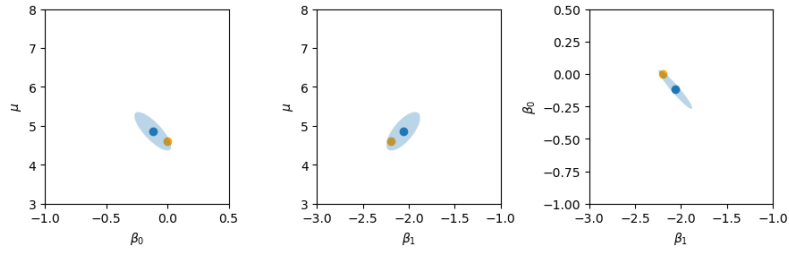
Because the empirical distribution F_k of $\{b_{[j]} : j \in \mathcal{I}_k\}$ satisfies $|\mathbb{E}_{F_k}[\|b_{[j]}\|_2^2] - m^{(2)}(\mathcal{X}_k)| < \delta$ and $|\mathbb{E}_{F_k}[\|b_{[j]}\|_2^4] - m^{(4)}(\mathcal{X}_k)| < \delta$,

$$\begin{aligned} \frac{1}{N_k} \sum_{j \in \mathcal{I}_k} r_{d-1}(\|b_{[j]}\|_2^2, \underline{\chi}_k) &= \mathbb{E}_{F_k} r_{d-1}(\|b_{[j]}\|_2^2, \underline{\chi}_k) \leq \bar{\rho}_{m^{(2)}(\mathcal{X}_k), m^{(4)}(\mathcal{X}_k)}^{2\delta}(\underline{\chi}_k) \\ &\leq \underline{\rho}_{m^{(2)}(\mathcal{X}_k), m^{(4)}(\mathcal{X}_k)}^{2\delta}(\underline{\chi}_k) + (\bar{\rho}_{m^{(2)}(\mathcal{X}_k), m^{(4)}(\mathcal{X}_k)}^{2\delta}(\underline{\chi}_k) - \underline{\rho}_{m^{(2)}(\mathcal{X}_k), m^{(4)}(\mathcal{X}_k)}^{2\delta}(\underline{\chi}_k)) \\ &\leq \alpha + \sup\{\bar{\rho}_{m^{(2)}, m^{(4)}}^{\delta}(\chi) - \underline{\rho}_{m^{(2)}, m^{(4)}}^{\delta}(\chi) : \chi \in [0, \infty), (m^{(2)}, m^{(4)}) \in \mathcal{M}^{\mathcal{U}}\}, \end{aligned}$$

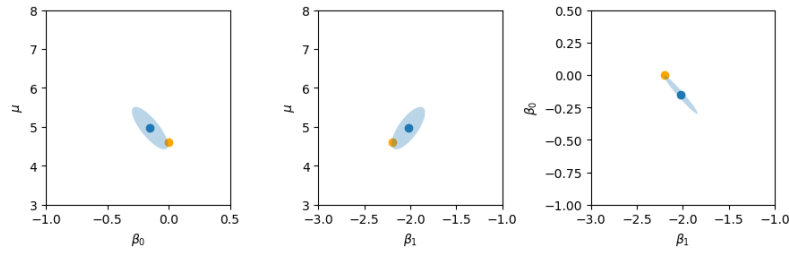
where the last term converges to 0 as $\delta \rightarrow 0$. Therefore, there exists $\delta > 0$ such that the last term is smaller than ϵ . By the δ , we can find the covering $\mathcal{X}_1, \dots, \mathcal{X}_K$, \bar{N}_k and then finally the desired $\bar{N}_{\mathcal{X}}$ so that $N_{\mathcal{X}} \geq \bar{N}_{\mathcal{X}}$ implies $\frac{N_{\mathcal{X}} - \bar{N}_{\mathcal{X}}}{N_{\mathcal{X}}} < \epsilon$ and

$$\mathbb{E} \left[\frac{1}{N_{\mathcal{X}}} \sum_{j \in \mathcal{I}_{\mathcal{X}}} \mathbb{I}\{\theta_{[j]} \notin \widetilde{\mathcal{C}}_{[j]}\} \middle| \theta_{[1, \dots, N]}, \Upsilon_{[1, \dots, N]} \right] \leq \alpha + 3\epsilon.$$

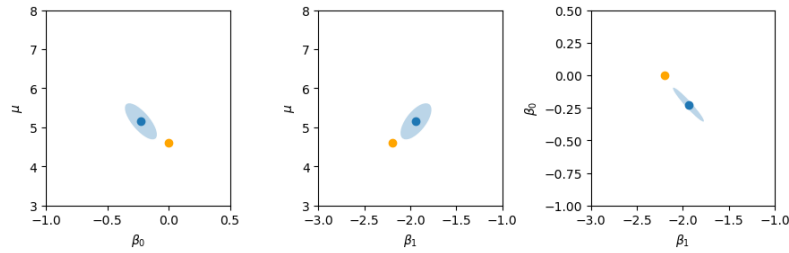
C. Appendix: Supplementary Figures



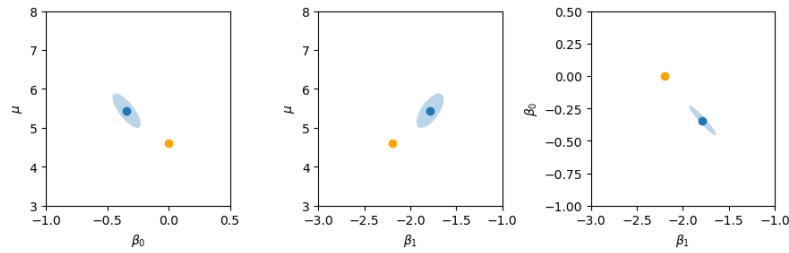
(a) Bayesian estimates using the least informative prior with $\sigma = 1/2$



(b) $\sigma = 3/8$



(c) $\sigma = 1/4$



(d) Bayesian estimates using the most informative prior with $\sigma = 1/8$

Fig. 12. True model parameters (orange), and Bayesian estimates (blue), together with 95% credible intervals (light blue) using four priors. The infection and death processes were simulated like in Fig. 3. The model in Eqs. (3) and (4) was fitted using Bhatt et al. (2023) with priors $N(0, \sigma)$ priors for β_0 and β_1 , where (a) $\sigma = 1/2$ (corresponding to the least informative priors), (b) $\sigma = 3/8$, (c) $\sigma = 1/4$ and (d) $\sigma = 1/8$ (corresponding to the most informative priors).

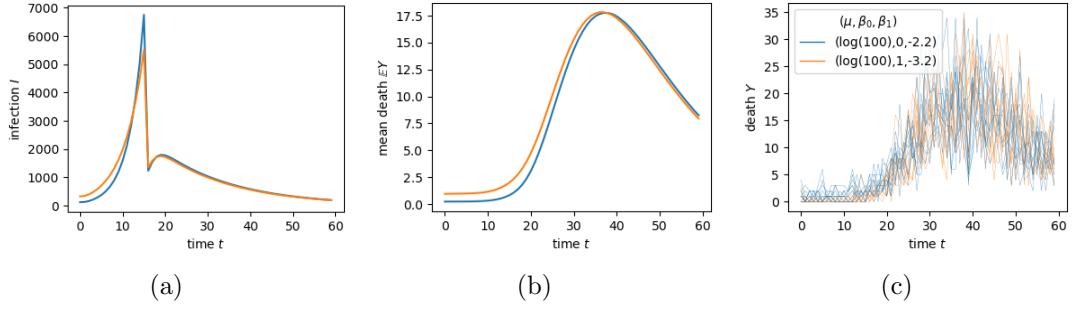


Fig. 13. (a) Mean infection and (b) death curves simulated from Eqs. (3) and (4) with $(\mu, \beta_0, \beta_1) = (\log(100), 0, -2.2)$ (blue) and $(\log(25), 1, -3.2)$ (orange), and (c) ten death processes simulated from each of these models, assuming NB distributions. The observed data look very similar for the two values of (μ, β_0, β_1) : it would be difficult to pick priors for (μ, β_0, β_1) by looking at the data.

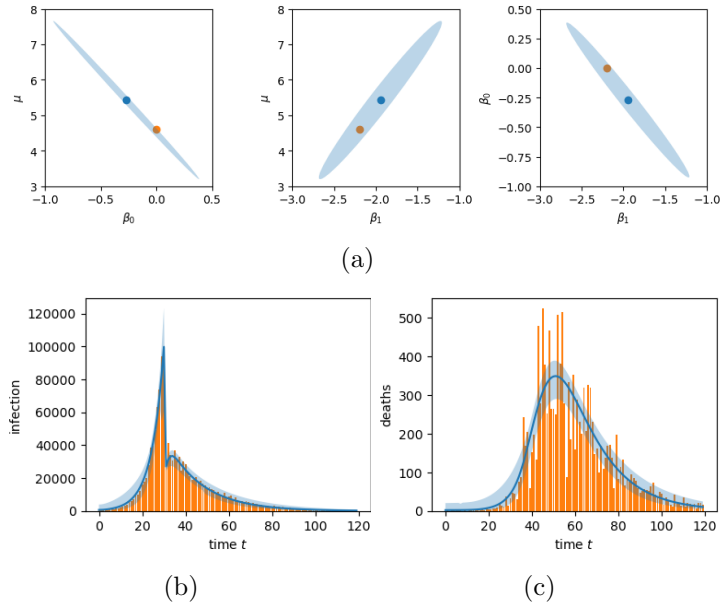


Fig. 14. Gaussian model fitted by ML to NB data. True quantities (model parameters, simulated infections and deaths) are in orange; ML estimates estimates are in blue with 95% confidence intervals (light blue). The infection and death processes in (b,c) were simulated from NB distributions with means in Eq. (1), R_t in Eq. (3), true parameters $\mu = \log(100)$, $\beta_0 = 0$ and $\beta_1 = -2.2$ in (a), and binary intervention process $A_t = 0$ for $t < 30$ and $A_t = 1$ for $t \geq 30$. The model in Eqs. (3) and (4) was fitted assuming Gaussian distributed deaths. The diagnostics for this fit are in Fig. 9.

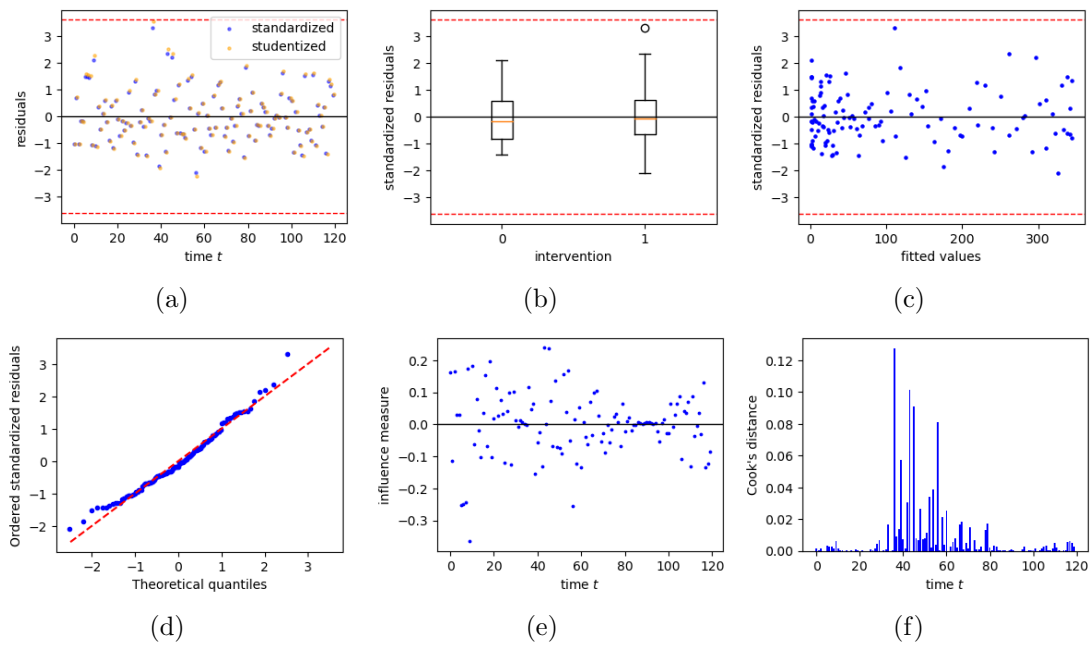


Fig. 15. Diagnostics for the NB model fitted to the NB data shown in Fig. 3. (a) Standardized and studentized residuals versus t . (b) Standardized residuals versus A_t and (c) versus \hat{Y}_t . (d) QQ plot of standardized residuals. (e) Influence on $\hat{\beta}_1$ and (f) Cook's distance, versus t . All diagnostics look fine.

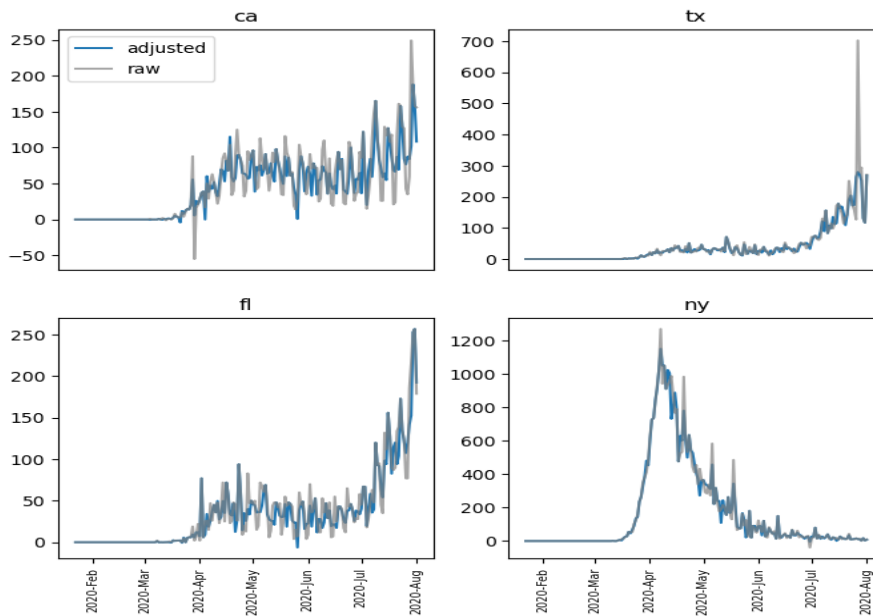


Fig. 16. Observed and weekend corrected death time series for four representative states. The large grey spikes lying above the blue curves are the monday effects, and those below are the weekend effects.

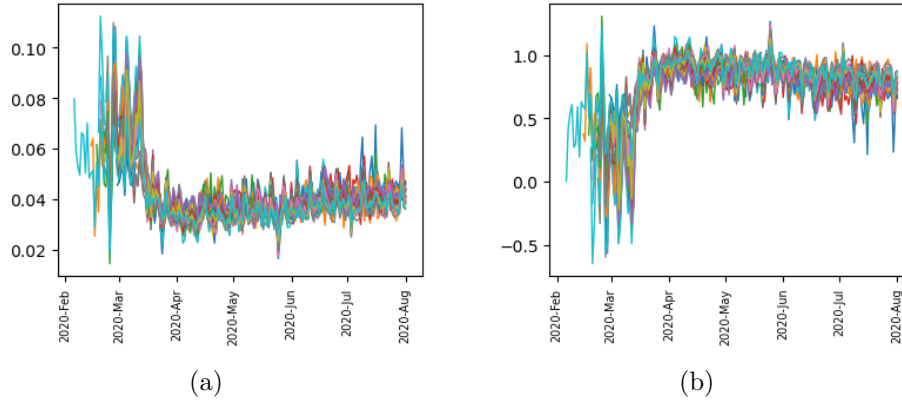


Fig. 17. Rescaling and shifting mobility A_t . (a) Observed Mobility time series in the 30 states and (b) scaled and shifted versions so the new values are mostly in the $[0, 1]$ range. The ML estimates of β_1 on the original scale are around 100. When we rescale A_t , the β_1 estimates have approximately the same magnitude and sign as in Bhatt et al. (2023).

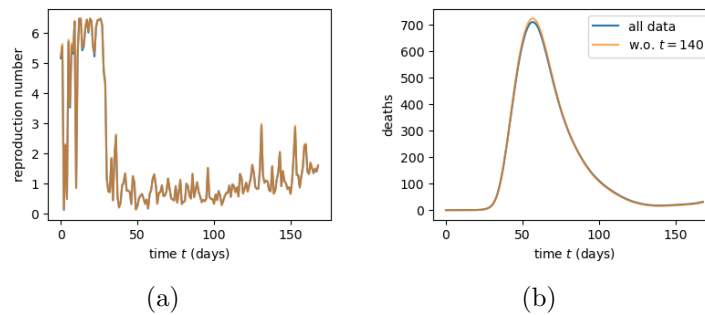
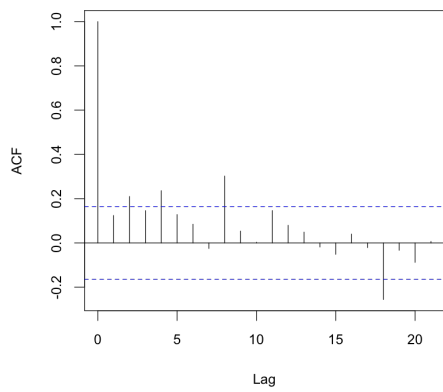
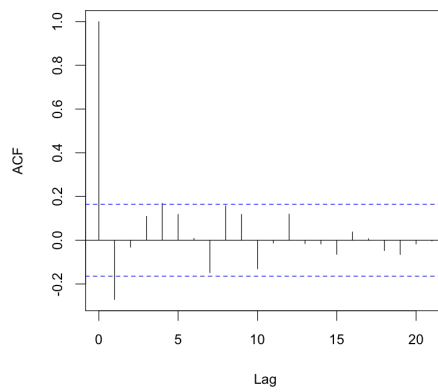


Fig. 18. Influence of Y_{140} for NY deaths. (a) Fitted reproduction numbers R_t and (b) mean fitted deaths with and without Y_{140} . The curves are nearly identical. The data and model fit in NY are in Fig. 8 and diagnostics are in Fig. 9.



(a)



(b)

Fig. 19. Autocorrelation function (ACF) of NY state residuals in Section 7.2. (a) ACF using standardized model residuals. The positive correlations for small lags may be due to the model lack of fit seen in Fig. 9(a). (b) ACF using first differences, which does not rely on a model. There does not appear to be long range correlations in (a) or (b), which is a condition for Theorem 5.7. ACFs for the other states are similar.